Reanalysis of the longest mass balance series in Himalaya using a nonlinear model: Chhota Shigri Glacier (India)

Mohd. Farooq Azam[1], Christian Vincent[2], Smriti Srivastava[1,3], Etienne Berthier[4], Patrick Wagnon[2], Himanshu Kaushik[1], Arif Hussain[1], Manoj Kumar Munda[1], Arindan Mandal[5], and Alagappan Ramanathan[6]

[1]*Department of Civil Engineering, Indian Institute of Technology Indore, Simrol, India-453552*
[2]*Univ. Grenoble Alpes, IRD, CNRS, INRAE, Grenoble INP, IGE, F-38000 Grenoble, France*
[3]*Department of Geography, University of Utah, Salt Lake City, USA*
[4]*Université de Toulouse, LEGOS (CNES/CNRS/IRD/UT3), Toulouse, 31400, France*
[5]*Interdisciplinary Centre for Water Research, Indian Institute of Science, Bengaluru 560012, India*
[6]*School of Environmental Sciences, Jawaharlal Nehru University, New Delhi-110067, India*

Correspondence to: Mohd. Farooq Azam (farooqazam@iiti.ac.in; farooqaman@yahoo.co.in)

Abstract

The glacier–wide mass balance (MB) series on Chhota Shigri Glacier has been reanalysed by combining the traditional MB reanalysis framework and a nonlinear MB model. The nonlinear model is preferred over the traditional glaciological method to compute the glacier–wide MBs as the former can capture the spatiotemporal variability of point MBs from a heterogeneous in-situ point MB network. Further, the nonlinear model is also used to detect erroneous measurements from the point MB observations over 2002–2023. ASTER and Pléiades stereo-imagery show limited areal changes but negative mass balances of -0.38 ± 0.05 m w.e. a^{-1} during 2003–2014 and -0.51 ± 0.06 m w.e. a^{-1} during 2014–2020. The nonlinear model outperforms the traditional glaciological method and agrees better with these geodetic estimates. The reanalysed mean glacier–wide MB over 2002–2023 is -0.47 ± 0.19 m w.e. a^{-1}, equivalent to a cumulative loss of -9.81 ± 0.87 m w.e. Our analysis suggests that the nonlinear model can also be used to complete the MB series if for some years the field observations are poor or unavailable. With this analysis, we revisit the glacier-wide MB series of Chhota Shigri Glacier and provide the most accurate and up-to-date version of this series, the longest continuous ever recorded in the Himalaya. We recommend applying the nonlinear model on all traditional glaciological mass balance series worldwide whenever data is sufficient, especially in the Himalaya where in-situ data are often missing due to access issues.

1. Introduction

Glaciers are excellent indicators of changing climate; therefore, long-term glacier mass changes are observed to understand the impacts of climate change (Oerlemans, 2001; Zemp et al., 2019). Glacier monitoring is also essential to understand possible glacial hazards (Harrison et al., 2018; Shukla et al., 2018; Shugar et al., 2021; Gantayat and Ramsankaran, 2023), regional hydrology (Azam et al., 2021; Yao et al., 2022; Nepal et al., 2023), and sea level rise (Gardner et al., 2013; Rounce et al., 2023). The glacier mass balance (MB) can be estimated from satellite data, through modelling approaches or measured using the field-based traditional glaciological method (Cogley, 2009; Zemp et al., 2015; Kumar et al., 2018; Miles et al., 2021; Berthier et al., 2023).

Over the last decade, rapid development has been made through satellite geodetic MB estimates covering almost all glacierized areas in the Himalaya (Brun et al., 2017; Bolch et al., 2019; Shean et al., 2020; Hugonnet et al., 2021; Jackson et al., 2023). These geodetic estimates are primarily available at a multiannual scale and thus cannot be used to study the inter-annual variability in glacier MB. Conversely, field measurements using standard methods (Østrem and Stanley, 1969) yield data on the seasonal/annual response of glacier MB to local meteorological conditions (Zemp et al., 2015). Field MB observations remain scarce in the Himalaya compared to the other mountain ranges (Azam et al., 2018) and have been limited to only 35 glaciers (Vishwakarma et al., 2022). Most observations are available from easily accessible and small glaciers for short periods, generally less than 10-15 years. The ongoing MB series include Chhota Shigri, Hoksar, Kolahoi and Sutri Dhaka glaciers in the western Himalaya (Oulkar et al., 2022; Mandal et al., 2020; Romshoo et al., 2022; 2023), Mera, Pokalde, Rikha Samba, Trambau, West Changri Nup, Yala glaciers in the central Himalaya (Sunako et al., 2019; Wagnon et al., 2021; Stumm et al., 2021), and Ganju La and Thana glaciers in the eastern Himalaya (Tshering and Fujita, 2016).

For annual glacier–wide MB estimation, the traditional glaciological method has been used in the Himalaya (Azam et al., 2018). This method involves interpolation/extrapolation of point MB measurements from fixed locations to the whole glacier area by applying different approaches, including contouring, profiling, and kriging (Østrem and Brugman, 1991; Zemp et al., 2013) or application of observed MB gradients to the glacier hypsometry (Funk et al., 1997; Wagnon et al., 2021). The selected point measurement sites may not be representative of the surrounding areas because (1) ablation stakes are often inserted away from the steep slopes towards the valley walls for safety reasons; thus, snow avalanche inputs

onto valley glaciers are not included; (2) crevassed areas are not sampled, (3) snow accumulation is site-specific and largely depends on local topography that controls snow drift and deposition and (4) harsh weather sometimes restricts access to accumulation measurement sites. Almost all the MB series are victims of one or other such issues; therefore, the estimated glacier–wide MBs often carry systematic biases (Thibert et al., 2008). These biases can be corrected by calibrating the MB series using satellite-derived geodetic mass estimates generally over 5-10 years (Zemp et al., 2013; Wagnon et al., 2021).

Furthermore, it is practically difficult to keep the position fixed for point measurements due to accessibility issues, stake displacement due to glacier dynamics, use of different surveying equipment (GPS, dGPS, total station, theodolite, etc.) and different researchers' involvement for decades of monitoring. Hence, the measurement network differs in space and time. In this situation, heterogeneous in-situ measurements do not always allow to catch the large spatiotemporal variability of point MBs within the same elevation range (Funk et al., 1997; Vincent and Six, 2013); consequently, the point MB-elevation relationship is insufficient to investigate the changes in glacier–wide MBs (Kuhn, 1984; Huss and Bauder, 2009; Thibert et al., 2013).

To include the spatiotemporal variability of point MB measurements, Lliboutry (1974) proposed a linear statistical model and tested it over the small ablation area of Saint Sorlin Glacier (France), assuming similar temporal changes of the MB over the whole area. Vincent et al. (2018) suggested that the linear model of Lliboutry (1974) was valid over a limited elevation range but ignored the decreasing spatiotemporal variability of point MBs with elevation (Oerlemans, 2001). To address this issue, they proposed a nonlinear model that considers the decreasing spatiotemporal changes in point MBs over the large elevation range and successfully tested their model on four different glaciers from different climate regimes, including Chhota Shigri Glacier (India).

The MBs on Chhota Shigri Glacier were estimated using the nonlinear model over 2002–2016 and then calibrated using geodetic MB over 2005–2014 (Vincent et al., 2018). In the present study, we extended the MB series on Chhota Shigri Glacier up to 2023 using the traditional method, estimated the areal changes and geodetic MBs over the 2003–2014 and 2014–2020 periods, estimated the debris cover as of September 2020, and reanalysed the annual MB series since 2002 using a novel reanalysis framework that combines the Vincent et al. (2018) nonlinear model and the reanalysis framework proposed by Zemp et al. (2013). Additionally, we assessed areal changes and geodetic MBs of neighbouring glaciers Hamtah and Sichum over the same periods based on available satellite stereo-images.

Since 2002, the MB series of Chhota Shigri Glacier has been continuously monitored, making it the longest series in the Himalaya. Azam (2021) highlighted the importance of Chhota Shigri as a reference glacier for large-scale MB and hydrological studies; therefore, the main aim of the present study is to produce the most accurate glacier–wide MB series in this region. First, the nonlinear model of Vincent et al. (2018) was used to detect the erroneous point MB measurements in the dataset. Second, the nonlinear model was applied using the observed point MBs to estimate the glacier–wide MB at an annual scale. Third, homogenization of the glacier–wide MB series accounting for glacier areal changes was performed; and fourth, the glacier–wide MB series was calibrated using geodetic MBs. Additionally, we compared the performance of the nonlinear model with the traditional method for estimating glacier–wide MB. We also assessed the nonlinear model's ability to estimate glacier–wide MB using end-of-season snowline data when field measurements were unavailable in a particular year.

2. Study area

Chhota Shigri Glacier (32.28° N, 77.58° E) is in the Chandra River Basin, a tributary of Upper Indus Basin, Lahaul-Spiti valley of the western Himalaya (Fig. 1). Chhota Shigri flows from 5830 to 4100 m a.s.l., with a length of ~9 km and an area of 15.47 km^2 (in 2020). Based on the most updated map obtained in September 2020, 12% of its total surface area is covered with debris between the snout and 4500 m a.s.l., including medial and lateral moraines from 4100 to ~4900 m a.s.l. and a debris-covered eastern tributary glacier (Fig. 1). Debris thickness ranges from less than a few centimetres of thin debris to a few meters of boulders. Valley walls bound its accumulation area, with the highest Devachan peak (6250 m a.s.l.). The accumulation area has two east- and west-oriented tributaries that feed to the main ablation area (<5070 m a.s.l.), having a north aspect and divided into two parallel flows by a medial moraine.

128
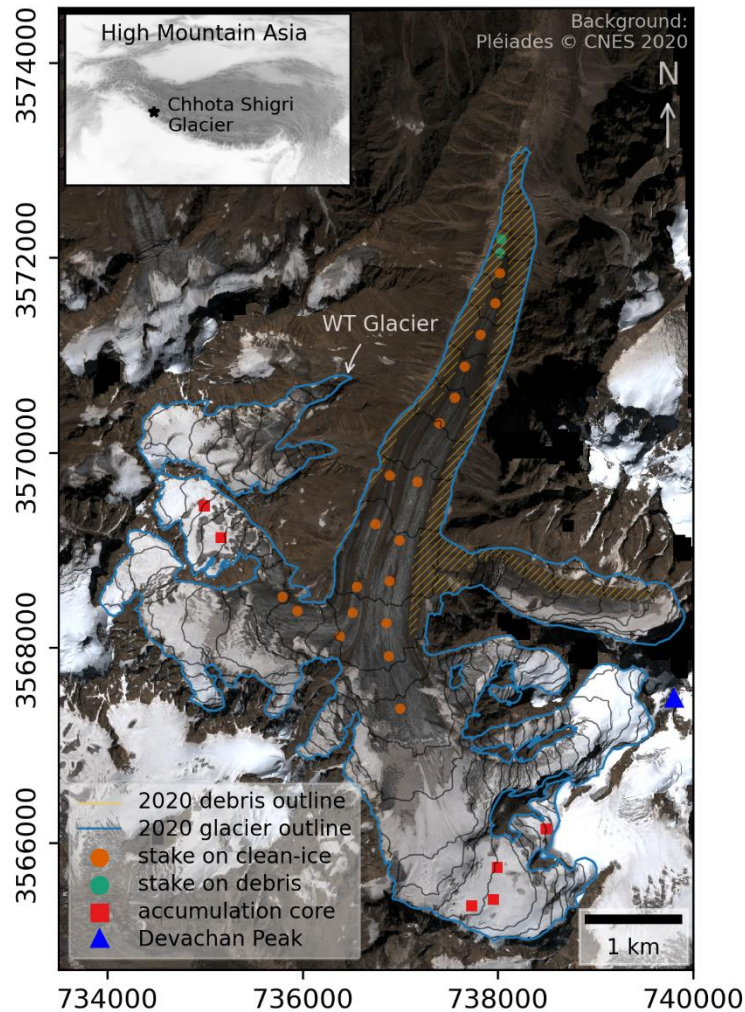
Figure 1: Chhota Shigri Glacier showing the location of ablation and accumulation point measurement sites. Orange strips show the debris-covered glacier area. The background image is a Pléiades satellite image taken on 12 September 2020 (Copyright CNES 2020, Distribution Airbus Defence and Space). The glacier extent corresponds to 12 September 2020. The coordinates are in UTM North, Zone 43.

Chhota Shigri is a well-studied glacier for various aspects, including traditional MBs, energy balance, dynamics, ice thickness, hydrology, etc. (Wagnon et al., 2007; Azam et al., 2012; Ramsankaran et al., 2018; Haq et al., 2021; Srivastava and Azam, 2022a; Mandal et al., 2020, 2022). Several studies have also observed its geodetic MBs (Berthier et al., 2007; Vincent et al., 2013; Brun et al., 2017; Mukherjee et al, 2018). Long-term annual MBs have been reconstructed over 1950–2020 applying a temperature index model (Srivastava et al., 2022) and over 1979–2020 using an energy balance model (Srivastava and Azam, 2022b). Due to recent glacier wastage on Chhota Shigri Glacier, the western tributary (WT) glacier got disconnected in the summer of 2012 (Srivastava et al., 2022). The fragmented tributary is now clearly visible in the high-resolution Pléiades image from 12 September 2020 (Fig. 1).

145   In this study, we focus on Chhota Shigri Glacier, but the available satellite stereo-
146   images also cover neighbouring Hamtah and Sichum glaciers; therefore, we also estimated
147   the areal changes and geodetic MBs for these two glaciers (sections 3.4 and 3.5). Hamtah
148   Glacier has been studied for its MBs and avalanche contribution (Vincent et al., 2013; Laha
149   et al., 2017). Further, for all three glaciers, we also delineated the debris cover corresponding
150   to 2020 (Table 1).

3. Methods

3.1 Traditional mass balance method

153   Glacier–wide annual MBs (B_a) have been estimated using a network of 22-25 ablation
154   bamboo stakes (inserted up to 10 m into the glacier) distributed over 4300-4900 m a.s.l. along
155   the main axis of the glacier (Fig. 1), and 4-6 accumulation pits/cores over 5160-5550 m a.s.l
156   distributed over the eastern and western tributaries of the glacier (Wagnon et al., 2007). The
157   traditional glaciological profile method was used to estimate the glacier–wide MB from the
158   observed point MBs (Østrem and Stanley, 1969). First, using the observed point MBs, the
159   mean altitudinal MBs were estimated for each 50-m elevation band from available point MBs
160   within each elevation band (Fig. 1). In case no measurements were available (due to loss of
161   stakes or missing accumulation measurements) the MBs were estimated using linear
162   interpolation/extrapolation of neighbouring bands. Second, the B_a (in m w.e. a^{-1}) was
163   estimated as follows:

$$B_a = \frac{1}{S} \sum_{z=min}^{z=max} b_z s_z, \qquad (1)$$

165   where b_z is the mean altitudinal MB (in m w.e. a^{-1}) of a given elevation band, z, of area s_z
166   (m^2) and S is the total glacier area (m^2). In the ablation area, emergence changes at each
167   ablation stake were converted to the point MB using a fixed density of 900 kg m^{-3} for ice and
168   350 kg m^{-3} for snow (Wagnon et al., 2007; Cogley et al., 2011), while in the accumulation
169   area, the varying snow/firn/ice densities (350-900 kg m^{-3}) were measured in the field. The
170   hydrological year for MB calculations is defined from 1 October to 30 September of the
171   following year; however, the exact measurement dates on site varied from a couple of days to
172   a week. Following Thibert et al. (2008), an overall uncertainty of ± 0.40 m w.e. a^{-1} for
173   glacier–wide MB was estimated by incorporating the errors in point measurements and their
174   distribution over the glacier (Azam et al., 2012).

175   Due to access difficulties, snowstorms like on 22-24 September 2018, or logistical or

176   budget issues, a limited number of point MB measurements could be carried out in some

177   years. This was the case for October 2015, when only two accumulation measurements could

178   be performed, or 2018, when measurements were done early in the season, before the storm.

179   For those two years, point MB data in the accumulation zone, where no measurements had

180   been taken, was estimated using previous years with a similar ablation pattern (Mandal et al.,

181   2020). In 2020, only two in-situ point MB data are available, preventing the traditional

182   method from being applied. Further, no measurements could be performed in 2021; hence, no

183   MB could be estimated. Supplementary Table S1 provides all information about the point

184   MBs and field expeditions since 2002.

3.2 Nonlinear mass balance model

186   The nonlinear MB model suggests that the observed point MB, $b_{i,t}$, at any site i for year t, can

187   be decomposed into (1) a spatial effect term, α_i, and (2) a temporal term, β_t, combined with a

188   spatial effect, γ_i, and can be written as (Vincent et al., 2018):

189
$$b_{i,t} = \alpha_i + \beta_t\gamma_i + \varepsilon_{i,t}, \qquad (2)$$

190   where α_i, the spatial effect at location i, is the average point MB at the site over the whole

191   study period, β_t is the annual deviation from the average point MB (thus $\Sigma\ \beta_t = 0$), and $\gamma_i =$

192   σ_i/σ_{max} is a scaling factor defined as the ratio of the standard deviation of annual MB at site i

193   and the maximum standard deviation (σ_{max}) observed from the point MB measurements over

194   a long period. The $\varepsilon_{i,t}$ term represents residuals resulting from measurement errors and

195   inconsistencies between the model and observed data. The spatiotemporal decomposition

196   proposed in equation 2 assumes that β_t is the same at all point locations for any given year (t)

197   and thus has a glacier–wide significance while γ_i term accounts for nonlinear effects with

198   elevation (Vincent et al., 2018).

199   To compute the scaling factor, γ_i, on Chhota Shigri Glacier, standard deviations were

200   computed from the point MBs available for each 50-m elevation band as the point MBs are

201   not available each year from the same fixed locations (Fig. 2). The standard deviations were

202   computed only for 50-m elevation bands where mean annual MBs were available from in-situ

203   measurements over a minimum of ten years, and it was assumed that the computed standard

204   deviations are representative of the whole period of investigation (2002-2023). This resulted

205   in 16 standard deviation values over the whole glacier with a maximum standard deviation of

206   1.17 m w.e. a^{-1} at 4525 m a.s.l. (4500-4550 band) and a minimum standard deviation of 0.40

207 m w.e. a^{-1} at 5325 m a.s.l. The decreasing magnitude of standard deviation with elevation

208 indicates the decreasing sensitivity of the annual MB to temperature and precipitation (Fig.

209 2), as already suggested by several studies on glaciers worldwide (Kuhn, 1984; Soruco et al.,

210 2009; Basantes-Serrano et al., 2016; Vincent et al., 2018; Wagnon et al., 2021). The

211 measurements are poor in the accumulation area, and no measurement was available above

212 5325 m a.s.l.; therefore, after some trials, we adjusted the standard deviation at 6000 m a.s.l.

213 to be zero (Fig. 2). A decreasing trend in standard deviation values below 4525 m a.s.l. (Fig.

214 2) is due to the presence of debris cover over the tongue of Chhota Shigri Glacier (Fig. 1) that

215 undermines the glacier's sensitivity to climate (Vincent et al., 2013; Banerjee and Shankar,

216 2013). The scaling factor, γ_i, at each point MB location, was computed from the 2-degree

217 polynomial function, fitted over the standard deviation vs elevation scatter plot (Fig. 2).
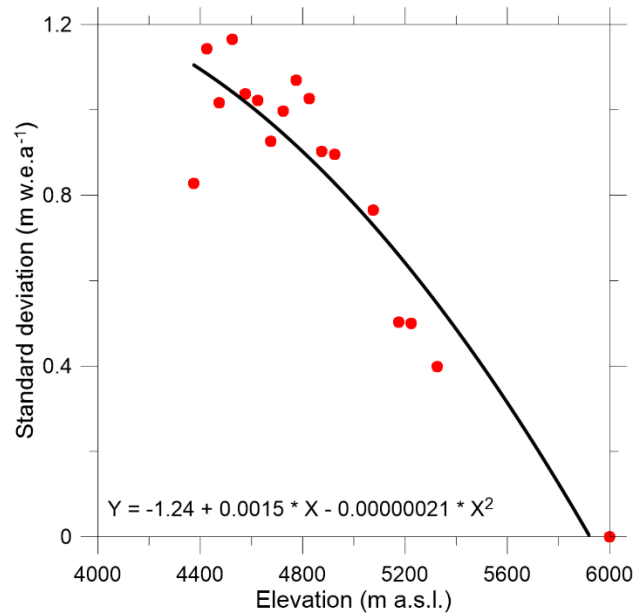
218

219 **Figure 2:** Standard deviations of the annual MBs versus elevation. The black line
220 corresponds to a polynomial fit (degree of freedom = 2). The standard deviations were
221 estimated for those 50m elevation bands where a minimum of 10 years of point
222 measurements were available at each site, and it is assumed to be zero at 6000 m a.s.l. (above
223 the glacier top at 5830 m a.s.l.).

224

225   The nonlinear model was run at 200m x 200m spatial resolution over 2002-2023

226 using all available point MBs (413-point measurements, excluding the erroneous

227 measurements, section 3.3) and polynomial equation (Fig. 2; details can be found in SI of

228 Vincent et al., 2018). The MB is assumed to be spatially constant over each 200m x 200m

229 grid for a given year. If there is more than one observation in a grid in a given year, then the

230 mean MB of the available observations was used for MB computation. The grid size is a

231 compromise between the spatial variability and the density of available point measurements.

Field measurements were unavailable in the 2020/21 year (section 3.1); hence, the nonlinear model cannot be run for this hydrological year. To run the model, at least one point MB measurement is required each year (Vincent et al., 2018). We assumed the snow line altitude (SLA) at the end of the ablation season to be equivalent to the equilibrium line altitude (ELA) (Rabatel et al., 2005; Brun et al, 2015; Davaze et al., 2020; Barandun et al., 2021). The SLA was delineated on a 6 September 2021 Sentinel image, and zero MBs (MB at ELA = 0 m w.e.) were assumed for two 200m x 200m grids where MB observations were available from other years (Fig. 3). It should be noted that there was no other cloud-free image from September 2021. The MB estimation from SLA using the nonlinear model is discussed in detail in section 5.3.
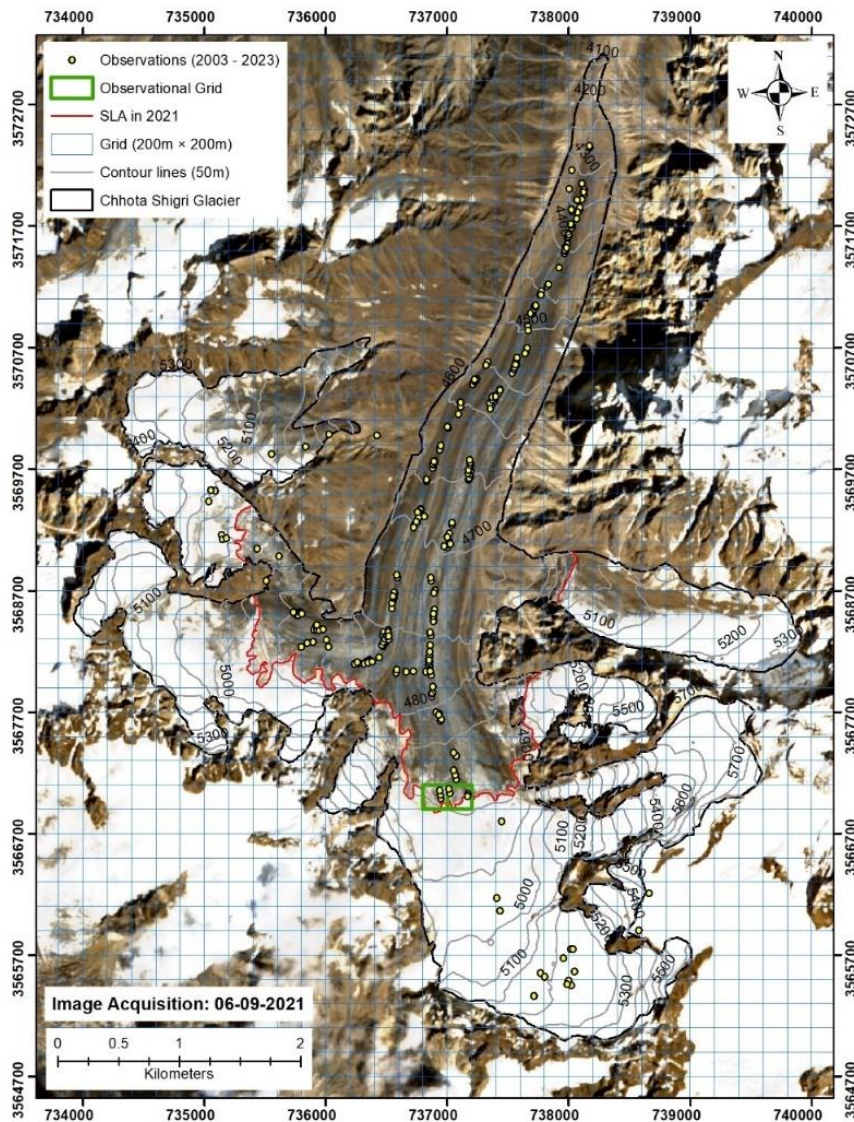
Figure 3: Distribution of all 413-point MB measurements (yellow dots) available over 2002-2023 on Chhota Shigri Glacier. The grids (in light blue) show a spatial resolution of 200m x

245 200m of the nonlinear model. For 2020/21, no field measurement was conducted; hence, two
246 grids (shown with green colour outline) corresponding to zero MB were selected on the
247 delineated SLA to run the model. The background is a Sentinel image from 6 September
248 2021, which is used to delineate the SLA.

249   The model output provides the mean α_i and mean γ_i for each point location over
250 2002–2023, and β_t for each year (equation 2). Fifty-four values for α_i and γ_i, and 21 values
251 for β_t (corresponding to each hydrological year) were computed (Table S2 and S3). For the
252 calculation of glacier–wide MB, a spatial distribution of α_i over the whole surface area of the
253 glacier is needed. First, for each 50-m elevation range (e), mean α_e was estimated from all
254 available α_i by taking a simple arithmetic mean and γ_e from all available γ_i from respective
255 elevation bands (equation 2). The modelled point MBs were available over the 4355–5512 m
256 a.s.l. elevation range and beyond this range, the mean α_e and γ_e from the lowest (4300–4350
257 m a.s.l.) and highest (5500–5550 m a.s.l.) ranges were used to cover the lowest (0.15 km^2;
258 0.97% of total area) and highest (0.68 km^2; 4.40% of total area) parts of the glacier. Second,
259 applying α_e, γ_e and β_t from all elevation bands in equation 1 along with corresponding
260 elevation areas, the annual glacier–wide MBs over 2002-2023 were estimated.

3.3 Tracking the erroneous in-situ point mass balances

262 The nonlinear model computes the residuals (difference between the measured and
263 theoretical values) of each measured point MB and can detect errors in in-situ point MB data
264 (Vincent et al., 2018). The distribution of residuals over the glacier as a function of distance
265 from the snout showed no spatio-temporal pattern (Fig. 4A), indicating that the nonlinear
266 model does not provide any apparent bias for any specific year. As expected, the residuals
267 followed a normal distribution with a standard deviation (STD) of 0.35 m w.e. a^{-1} (Fig. 4B).
268 To detect the measurement errors in the point MBs in the Chhota Shigri measurement
269 network over 2002–2023, we assumed all the point MBs having residuals >2STD (0.70 m
270 w.e. a^{-1}) to be suspicious. Of 423-point MB measurements, 15 such point MBs were found
271 and investigated further. Five-point MBs had been wrongly reported from the notebooks and
272 thus have been corrected. We could not find any reason for the rest of the suspicious points.
273 Therefore, they have been considered erroneous and discarded in the final model run. The
274 erroneous data were collected in different years (five ablation point measurements from 2009,
275 2012, 2018 and 2022, and five accumulation point measurements from 2009, 2011, 2014 and
276 2022) (Fig. 4). The standard deviation of the residuals from the nonlinear model was reduced
277 from 0.35 to 0.30 m w.e. a^{-1} after correction/removal of suspicious point MB measurements.
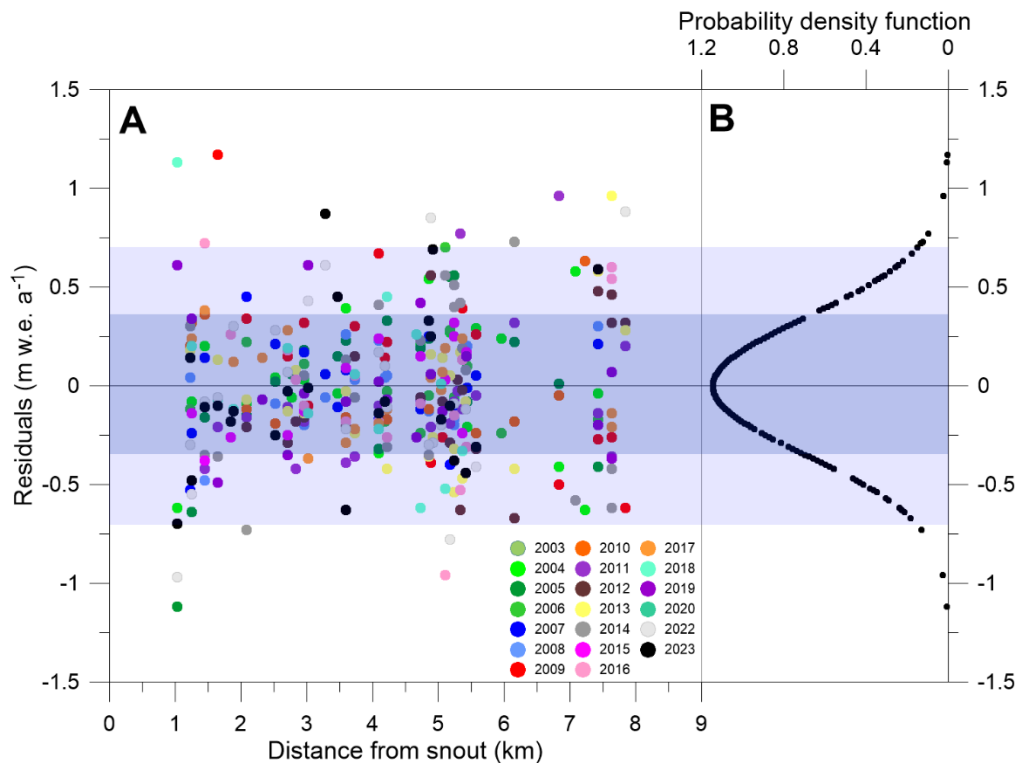
278

279 **Figure 4: (A)** Shows the residuals between measured and modelled point MBs from the
280 nonlinear model using all available 423-point MBs as a function of distance from the glacier
281 snout for each hydrological year between 2002 and 2023. The dark and light blue shaded
282 envelopes represent the 1 STD and 2 STD values, respectively. **(B)** the probability density
283 function (normal distribution curve) of all point MB residuals between 2002 and 2023.

284

285 **3.4 Areal changes and debris cover estimation**

286 The areal changes and debris cover were estimated on Chhota Shigri, Sichum and Hamtah
287 glaciers by manual delineation following the Global Land Ice Measurements from Space
288 (GLIMS) guidelines from the available ASTER (08/10/2003) and Pléiades images
289 (26/09/2014 and 12/09/2020) (Raup et al., 2007). We have preferred manual delineation as it
290 was considered the most accurate method for delineating glacier outlines (Stokes et al., 2007;
291 Garg et al., 2017; Shukla and Qadir, 2016). The ice divides were interpreted using the
292 Pléiades Digital Elevation model (DEM). The changes were estimated for the ablation area
293 for 2014 and 2020, as the changes in the accumulation area were insignificant. The generated
294 glacier outlines (2003, 2014 and 2020) were used to estimate the glacier area changes during
295 2003–2020. The uncertainties associated with the glacier area were calculated using the
296 buffer method (Bolch et al., 2010; Chand and Sharma, 2015). The buffer size was half the
297 pixel value (Bolch et al., 2010; Andreassen et al., 2022).

298 **3.5 Geodetic mass balances**

The geodetic MBs were estimated over two periods (2003–2014 and 2014–2020) for Chhota Shigri, Sichum and Hamtah glaciers using satellite stereo images from ASTER (15 m resolution) acquired on 08/10/2003 and Pléiades (0.70 m resolution) acquired on 26/09/2014 and 12/09/2020, respectively. The ASTER October 2003 stereo-pair was preferred to other ASTER or SPOT5 stereo pairs acquired in late summer 2002, 2004, and 2005 because it resulted in the smallest uncertainties. The stereo images were acquired close to the end of the hydrological year, reducing the impact of any seasonal offset. The DEM generation, co-registration and MB calculation procedure is the same as in Falaschi et al. (2023). Uncertainties for the glacier–wide geodetic MB were estimated using the patch method (Wagnon et al., 2021). This method aims to empirically determine the uncertainty associated with the mean elevation change by sampling patches of stable terrain of various sizes to measure the decay of the error with the averaging area.

Geodetic MBs were estimated over 10.97 years (from 08/10/2003 to 26/09/2014) and 5.96 years (from 26/09/2014 to 12/09/2020) and linearly scaled to estimate the geodetic MBs over 11- and 6-year periods, respectively to make a direct comparison with the in-situ MBs (estimated from end of September to end of September next year). Furthermore, the geodetic MBs included both the WT glacier, which fragmented around 2012 (Srivastava et al., 2022), and the main Chhota Shigri (area-weighted) (Table 1) for a direct comparison with the traditional and nonlinear MBs that include the WT glacier.

3.6 Homogenization of glacier–wide mass balances

In initial studies (Wagnon et al., 2007; Azam et al., 2012), a fixed hypsometry (glacier area and elevation) from SPOT5 2005 DEM was used, while in follow-up studies (Azam et al., 2014; Mandal et al., 2020) a fixed hypsometry from Pléiades August 2014 DEM was used to estimate the traditional MBs on Chhota Shigri Glacier. These fixed hypsometries insert bias in the MB series (Cogley et al., 2011; Zemp et al., 2013). Here, the Chhota Shigri Glacier annual MBs (from the traditional method and nonlinear model) are homogenized with the linearly changing annual hypsometries from ASTER and Pléiades DEMs over 2003–2014 and Pléiades DEMs over 2014–2020 (section 4.1). We adopted the approach suggested by Zemp et al. (2013) that assumes a linear area change over a record period (N years) and estimates the area (s) of an elevation band (e) for each year (t) as follows:

$$s_{e,t} = s_{e,0} + \frac{t}{N} \cdot (s_{e,N} - s_{e,0}), \qquad (3)$$

where $s_{e,0}$ and $s_{e,N}$ are the elevation bin areas from the first and the second geodetic survey, respectively, and the time t is zero in the year of the first survey. The homogenization process of both traditional and nonlinear MB series changed the annual glacier–wide MBs at most by 0.02 m w.e., reflecting the negligible impact of areal changes over the 2003–2020 period on Chhota Shigri Glacier (section 4.1). Post-2020, the hypsometry of the 2020 year was used to estimate the MBs till 2023. Figure 5 summarizes the overall methodology step-by-step, including homogenization, validation/calibration and error estimation (sections 3.7 and 3.9).
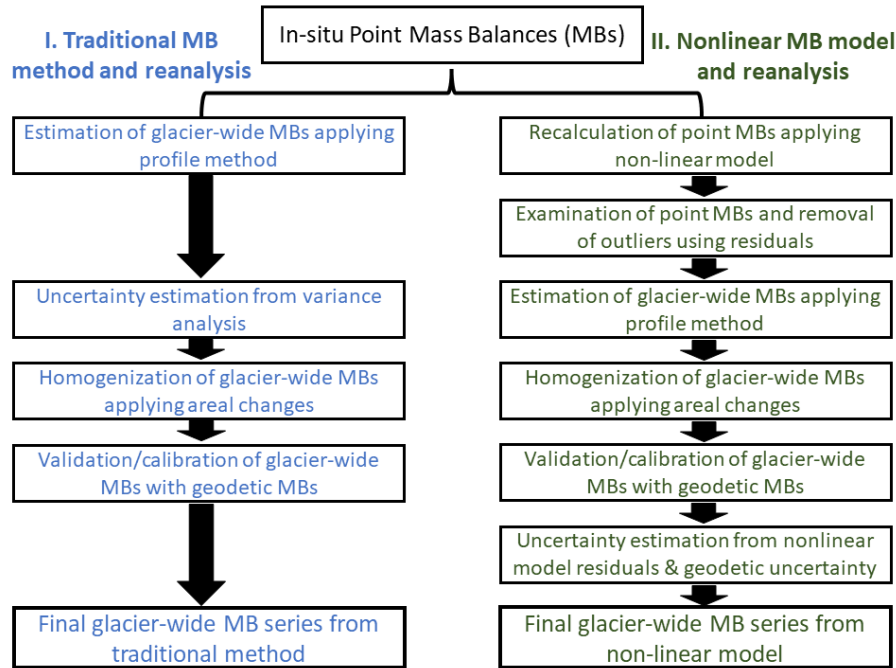
Figure 5: Conceptual diagram of the overall methodology: homogenization, uncertainty estimation, validation, and calibration steps.

3.7 Validation and calibration of glacier–wide mass balances

Previously, we validated the traditional MBs with geodetic MB available over 2005–2014 (Azam et al., 2016). The systematic biases were within the uncertainty ranges of traditional and geodetic MBs; hence, no calibration was done. In this study, we repeated this validation over two periods for which the geodetic MBs were calculated (section 4.2).

The traditional as well as nonlinear MBs over 2003–2014 were not statistically different from the geodetic MB, and the null hypothesis H_0 (the cumulative glaciological MB is not statistically different from the geodetic MB) was accepted at 95% and 90% levels (Zemp et al., 2013). However, over 2014–2020, both traditional and nonlinear MBs were statistically different from the geodetic MBs, and the null hypothesis H_0 was rejected at 95% as well as 90% levels. This showed that the systematic biases were significant over

2014–2020 (Table 2). Even though we did not observe a significant bias over 2003–2014, we decided to calibrate the traditional as well as nonlinear MBs over both periods as suggested in previous studies (Thibert et al., 2008; Huss et al., 2009; Andreassen et al., 2016; Wagnon et al., 2021).

In the calibration procedure, the annual relative variability of glacier–wide MBs is taken from the MB series and the series was fitted to the multi-annual geodetic MB, B_g, as follows:

$$B_{a,cal} = B_a + \frac{(B_g - \sum_N B_a)}{N}, \qquad (4)$$

where $B_{a,cal}$ is the annual calibrated glacier–wide MB and N is the number of years over which the geodetic MB has been estimated. It should be mentioned that the MBs obtained from traditional method or nonlinear model refer only to the surface MB, whereas the geodetic MBs also integrate the internal and basal MBs, assumed to be small compared to the surface MB (Cuffey and Paterson, 2010).

3.8 Calibration of mean altitudinal mass balances

The mean altitudinal MBs ($b_{e,t}$) for each 50-m elevation band (e) and each year (t) were computed using equation 1 exploiting the values of α_i, β_t and γ_i obtained from the nonlinear model. These altitudinal mean MBs were adjusted to fit the calibrated annual glacier–wide MBs following Zemp et al. (2013). The calibrated altitudinal mean MB ($b_{e,t,cal}$) for each year is estimated as:

$$b_{e,t,cal} = b_{e,t} - B_a + B_{a,cal}, \qquad (5)$$

where B_a is the uncalibrated annual nonlinear MBs and $B_{a,cal}$ is the calibrated annual nonlinear MBs. The equilibrium line altitude (ELA_{cal}) and MB gradient for each year (t) are also estimated by plotting the linear regression over the calibrated annual mean altitudinal MBs ($b_{e,t,cal}$) over an elevation range of 4375-5225 m. Finally, using the calibrated $ELAs$, the calibrated $AARs$ were estimated each year (Table 3).

3.9 Random error estimation in nonlinear mass balances

The random error ($\sigma_{B_{n,cal}}$) in calibrated nonlinear glacier–wide MB is estimated following:

$$\sigma_{B_{n,cal}} = \pm \sqrt{\frac{\sigma_{B_g}^2}{N} + \sum s_i^2 \, \sigma_\varepsilon^2}, \qquad (6)$$

382   σ_{B_g} is the error in the geodetic MBs (σ_{B_g} = 0.57 and 0.36 m w.e. a^{-1} over 2003–2014 and

383   2014–2020, respectively), N is the number of years for geodetic MB estimation (section 3.3),

384   s_i terms represent the relative areas of each 50-m elevation band (except for 5400-5850 m

385   a.s.l. range that has been treated as a single band) compared to the total glacier area (therefore

386     $\Sigma s_i = 1$), and σ_ε = 0.30 m w.e. a^{-1} is the standard deviation of the residual term of equation

387   (2) obtained with the nonlinear model (section 3.2). Equation 6 is valid for the hydrological

388   years within calibration periods (2003–2014 and 2014–2020). The random errors in nonlinear

389   glacier–wide MBs for 2002/03 and 2020–2023 hydrological years were estimated following

390   the procedure described in Wagnon et al. (2021). The mean annual random error, $\sigma_{B_{n,cal}}$, of

391   the calibrated nonlinear glacier–wide MB was estimated to be ±0.19 m w.e. a^{-1} over 2002-

392   2023, with slightly higher random errors for the years outside the calibration period (Table 3).

4. Results

4.1 Glacier area changes since 2003

395   Chhota Shigri, Sichum and Hamtah glaciers showed limited areal changes since 2003, mostly

396   restricted to the snout area (Table 1; Fig. 6). The estimated debris cover, corresponding to

397   September 2020 year, was 12%, 22% and 79% of the total area on Chhota Shigri, Sichum and

398   Hamtah glaciers, respectively (Table 1). During 2003–2020, the total area change for each

399   glacier was very small with a deglaciation rate of –0.07 ± 0.22 % a^{-1}, –0.07 ± 0.22 % a^{-1} and

400   –0.03 ± 0.19 % a^{-1} for Chhota, Sichum and Hamtah, respectively (Table 1).

4.2 Geodetic mass balances

402   The maps of elevation changes for 2003–2014 and 2014–2020 periods indicate a general

403   pattern of thinning for the glacier tongues and limited changes in the upper reaches of the

404   glaciers (Fig. 7). The area-weighted geodetic MB of Chhota Shigri Glacier (including WT)

405   was –0.43 ± 0.08 m w.e. a^{-1} over 2003–2020 (Table 1), with a higher annual wastage of –0.51

406   ± 0.06 m w.e. a^{-1} over 2014–2020 compared to –0.38 ± 0.10 m w.e. a^{-1} over 2003–2014

407   (Table 2). Sichum and Hamtah glaciers showed slightly stronger annual mass wastage of

408   –0.57 ± 0.08 and –0.51 ± 0.08 m w.e. a^{-1}, respectively over 2003–2020, with similarly an

409   increased mass wastage over the recent period (2014–2020) (Table 1). The slightly more

410   negative glacier–wide MBs on all these glaciers during 2014–2020 agree with a recent study

411   suggesting an increased wastage over the recent decade in the Himalaya (Hugonnet et al.,

412   2021).

413
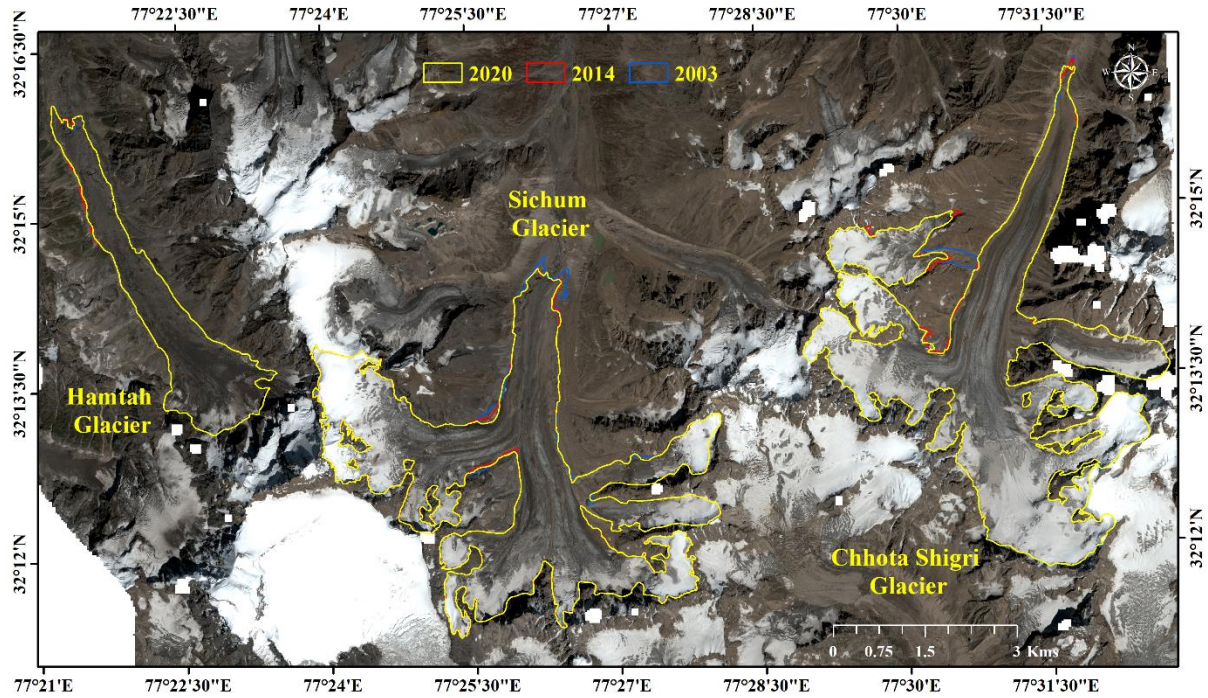
Figure 6: Glacier area change of Chhota Shigri, Sichum and Hamtah glaciers between 2003
and 2020 (Background image is Pleiades satellite imagery of 12 September 2020; CNES
2020, Distribution Airbus D&S).

417

Table 1: The areal and geodetic mass changes on Chhota Shigri, Sichum and Hamtah
glaciers over the 2003-2014 and 2014-2020 periods.

Time Period	2003-14	2014-2020	2003-2020
Chhota Shigri with WT (Area = 15.47 km², 12% debris cover in 2020)			
Area change (km²)	–0.15 ± 0.58	–0.05 ± 0.14	–0.20 ± 0.57
Area change rate (% a⁻¹)	–0.09 ± 0.33	–0.05 ± 0.15	–0.07 ± 0.22
Geodetic MB (m w.e.)	–4.18 ± 0.57	–3.08 ± 0.36	–7.26 ± 0.93
Geodetic MB (m w.e. a⁻¹)	–0.38 ± 0.10	–0.51 ± 0.06	–0.43 ± 0.08
Sichum (Area = 13.84 km², 22% debris cover in 2020)			
Area change (km²)	–0.14 ± 0.52	–0.02 ± 0.12	–0.16 ± 0.52
Area change rate (% a⁻¹)	–0.09 ± 0.34	–0.03 ± 0.14	–0.07 ± 0.22
Geodetic MB (m w.e.)	–6.07 ± 0.66	–3.68 ± 0.36	–9.75 ± 1.02
Geodetic MB (m w.e. a⁻¹)	–0.55 ± 0.09	–0.61 ± 0.06	–0.57 ± 0.08
Hamtah (Area = 4.12 km², 79% debris cover in 2020)			
Area change (km²)	–0.02 ± 0.13	–0.00 ± 0.03	–0.02 ± 0.13
Area change rate (% a⁻¹)	–0.05 ± 0.29	–0.01 ± 0.13	–0.03 ± 0.19
Geodetic MB (m w.e.)	–5.19 ± 0.55	–3.44 ± 0.36	–8.63 ± 0.91
Geodetic MB (m w.e. a⁻¹)	–0.47 ± 0.09	–0.57 ± 0.06	–0.51 ± 0.08

420
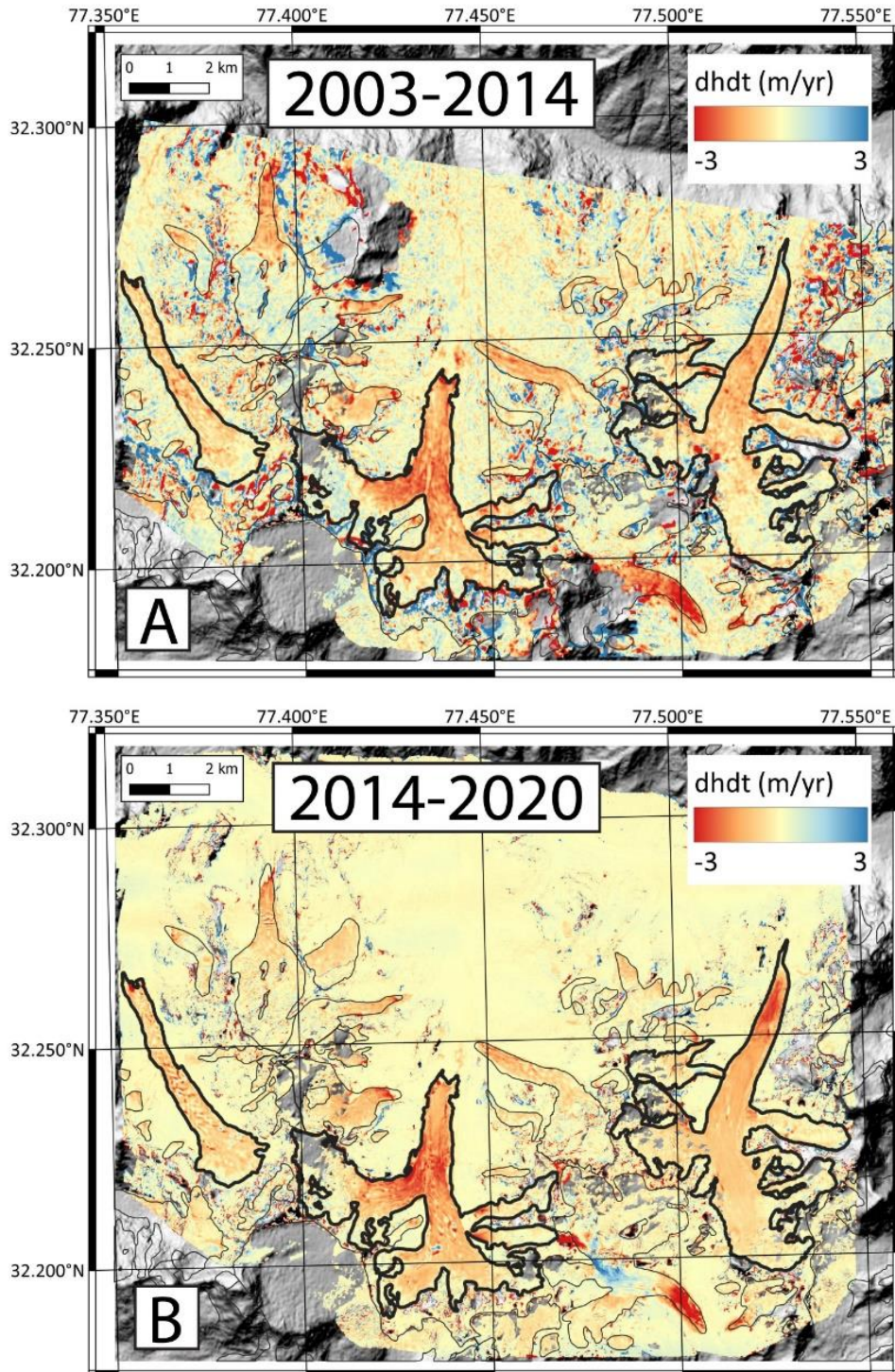
Figure 7: The thickness changes for Chhota Shigri, Sichum and Hamtah glaciers differencing the ASTER 2003 (08/10/2003) and Pléiades (26/09/2014) DEMs over 2003–2014 and Pléiades DEMs (26/09/2014 and 12/09/2020) over 2014–2020.

The mean annual geodetic mass wastage of -0.43 ± 0.08 m w.e. a^{-1} on Chhota Shigri Glacier over 2003–2020 is in good agreement with the region-wide mean glacier mass

426   wastage of -0.37 ± 0.15 m w.e. a^{-1} over the whole Lahaul-Spiti region (glacierized area =

427   7960 km^2) during a slightly different period (2000–2016), from multiple ASTER DEMs

428   (Brun et al., 2017). Hence, Chhota Shigri is a reference glacier in the Himalaya (Azam, 2021)

429   and a representative glacier for the whole Lahaul-Spiti region, as already suggested (Vincent

430   et al., 2013).

4.3 Annual and cumulative glacier–wide mass balances since 2002

432   Table 2 and Fig. 8 show the traditional and nonlinear MBs (before and after calibration) and

433   geodetic MBs over available periods. The traditional MBs were not available for 2019/20 and

434   2020/21 (section 3.1); therefore, to calibrate these MBs and to cover the geodetic

435   observations, the modelled MBs (2019/20 = 0.07 m w.e. and 2020/21 = –1.17 m w.e.) from

436   surface energy balance approach (Srivastava and Azam, 2022b) were added to the series.

437   Compared to uncalibrated traditional MB series, uncalibrated nonlinear MB series

438   showed much lesser biases with a slightly negative bias of –0.03 m w.e. a^{-1} (against a bias of

439   –0.10 m w.e. a^{-1} in traditional MBs) over 2003–2014 and of –0.17 m w.e. a^{-1} (against a bias

440   of 0.33 m w.e. a^{-1} in traditional MBs) over 2014–2020 (Table 2; Fig. 8). Therefore, following

441   equation 4, the nonlinear annual MBs were systematically increased by 0.03 m w.e. a^{-1} over

442   2003–2014 and by 0.17 m w.e. a^{-1} over 2014–2020 while traditional MBs were

443   systematically increased by 0.10 m w.e. a^{-1} over 2003–2014 and decreased by 0.33 m w.e. a^{-1}

444   over 2014–2020 to match the geodetic estimates (Fig. 8). The hydrological years 2002/03 and

445   2020–2023 are outside the calibration periods, but these years were also calibrated by the

446   mean values of biases observed over 2003–2014 and 2014–2020, respectively. To avoid

447   confusion, we discussed only the calibrated nonlinear glacier–wide MBs in the manuscript,

448   although the calibrated traditional MBs are given in Tables 2 and 3 for reference.

449   **Table 2:** Cumulative MBs (in parenthesis, mean annual MBs) from the traditional method,
450   nonlinear model, and geodetic estimates over available periods. The balance year 2002/03 is
451   not included here as it is not covered in the geodetic estimate available over 2003–2014. The
452   cumulative traditional MB over the 2014–2020 period has been estimated by adding the
453   modelled annual MB for 2019/20 (Srivastava and Azam, 2022b). All units are in m w.e. (m
454   w.e. a^{-1}).

	2003–2014	2014–2019	2014–2020
Traditional MB	–5.31 (–0.48)	–1.14 (–0.23)	–1.07 (–0.18)[*]
Nonlinear MB	–4.48 (–0.41)	–3.22 (–0.64)	–4.10 (–0.68)
Geodetic MB	–4.18 (–0.38)	-	–3.08 (–0.51)
Calibrated traditional MB	–4.18 (–0.38)	–2.82 (–0.56)	–3.08 (–0.51)
Calibrated nonlinear MB	–4.18 (–0.38)	–2.37 (–0.47)	–3.08 (–0.51)

455   [*]estimated from traditional MBs (2014-2019) and modelled MB (2019/20).

456
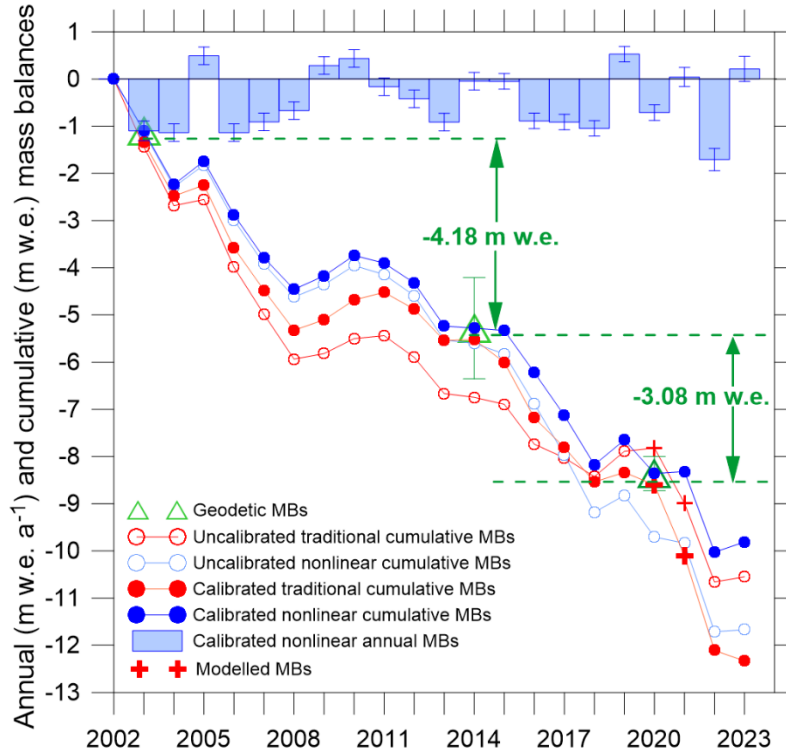
Figure 8: Calibrated nonlinear annual glacier–wide MBs (with random errors) over 2002–2023, traditional cumulative MBs over 2002–2023, nonlinear cumulative MBs over 2002–2023, calibrated nonlinear cumulative MBs over 2002–2023, calibrated traditional cumulative MBs over 2002–2023, and geodetic MBs over 2003–2014 and 2014–2020 (with estimated uncertainties). The cumulative traditional MB series (2002–2019) is completed till 2023 by adding the modelled MB of 2019/2020 and 2020/21 from Srivastava and Azam (2022b).

Table 3: Calibrated nonlinear MBs ($B_{a_{n,cal}}$), calibrated traditional MBs ($B_{a_{t,cal}}$), MB gradients (db/dz), ELA_{cal} and AAR_{cal} on Chhota Shigri Glacier between 2002 and 2023.

Year	Glacier Area (km²)	$B_{a_{n,cal}}$ (m w.e. a⁻¹)	Error of $B_{a_{n,cal}}$ (m w.e. a⁻¹)	$B_{a_{t,cal}}$ (m w.e. a⁻¹)	db/dz (m w.e. (100)⁻¹ a⁻¹)	ELA_cal (m a.s.l.)	AAR_cal (%)	Difference $B_{a_{n,cal}}$ - $B_{a_{t,cal}}$
2002/03	15.66	-1.10	0.21	-1.34	0.70	5145	33	0.24
2003/04	15.64	-1.14	0.19	-1.14	0.71	5156	32	0.01
2004/05	15.63	0.49	0.19	0.24	0.59	4911	67	0.26
2005/06	15.61	-1.14	0.19	-1.33	0.71	5157	32	0.19
2006/07	15.59	-0.91	0.19	-0.90	0.69	5128	36	-0.01
2007/08	15.57	-0.67	0.19	-0.84	0.67	5096	40	0.17
2008/09	15.56	0.29	0.19	0.22	0.60	4942	63	0.07
2009/10	15.54	0.43	0.19	0.42	0.59	4921	65	0.01
2010/11	15.52	-0.16	0.19	0.17	0.64	5022	50	-0.33
2011/12	15.50	-0.42	0.19	-0.36	0.66	5061	44	-0.06
2012/13	15.49	-0.91	0.19	-0.66	0.69	5131	34	-0.25
2013/14	15.47	-0.05	0.19	0.02	0.63	5004	53	-0.07
2014/15	15.46	-0.05	0.16	-0.48	0.64	5027	50	0.43
2015/16	15.45	-0.89	0.16	-1.18	0.70	5148	33	0.29
2016/17	15.44	-0.91	0.16	-0.62	0.70	5151	31	-0.29
2017/18	15.44	-1.05	0.16	-0.73	0.71	5167	30	-0.32
2018/19	15.43	0.53	0.16	0.21	0.60	4930	64	0.32
2019/20	15.42	-0.71	0.16	-0.26	0.69	5125	35	-0.45
2020/21	15.42	0.04	0.20	-1.49	0.63	5013	51	1.53
2021/22	15.42	-1.71	0.24	-2.00	0.76	5248	19	0.29
2022/23	15.42	0.21	0.27	-0.22	0.62	4985	56	0.44
Mean	**15.51**	**-0.47**	**0.19**	**-0.58**	**0.66**	**5070**	**44**	**0.12**
SD	**0.08**	**0.65**	**0.02**	**0.67**	**0.05**	**97**	**14**	**0.42**

466   *The calibrated traditional MBs for 2019/20 and 2020/21 years are originally from the model (Srivastava and Azam, 2022b).

467   The annual calibrated glacier–wide MB from the nonlinear model varied from 0.53 ±

468   0.16 m w.e. a^{-1} in 2018/19 to –1.71 ± 0.24 m w.e. a^{-1} in 2021/22 with a standard deviation of

469   0.65 m w.e. a^{-1} during 2002–2023 (Table 3). In the 21-year-long MB series, six hydrological

470   years (2004/05, 2008/09, 2009/10, 2018/19, 2020/21, and 2022/23 showed positive/near

471   steady state MBs. The mean annual glacier–wide MB was estimated to be –0.47 ± 0.19 m

472   w.e. a^{-1}, equivalent to a cumulative loss of –9.81 ± 0.87 m w.e. over 2002–2023 (Table 3).

473   The uncertainty in cumulative mass loss comes from error propagation law.

474   **4.4 Equilibrium line altitude and accumulation area ratio**

475   Using the calibrated mean altitudinal MBs (section 3.8), the equilibrium line altitude ELA_{cal},

476   accumulation area ratio AAR_{cal} and MB gradients (db/dz) were also estimated. The maximum

477   ELA_{cal} was 5248 m a.s.l. corresponding to the most negative MB of –1.71 ± 0.24 m w.e. a^{-1}

478   and minimum AAR_{cal} of 19% in 2021/22, while the minimum ELA_{cal} was 4911 m a.s.l.

479   corresponding to a positive MB of 0.49 ± 0.19 m w.e. a^{-1} and a maximum AAR_{cal} of 67% in

480   2004/05. The mean ELA_{cal} was 5070 m a.s.l. corresponding to a mean mass wastage of –0.47

481   ± 0.19 m w.e. a^{-1} and mean AAR_{cal} of 44% over 2002-2023.

482   The annual ELA_{cal} and AAR_{cal} showed good correlations with annual glacier–wide

483   MBs (r^2 = 0.98 and 0.97, respectively) over 2002-2023 (Fig. 5). The ELA_{cal} for a zero

484   glacier–wide MB (ELA_0) was also computed from the regression between glacier–wide MBs

485   and ELA_{cal} over 2002-2023 and calculated as ~5001 m a.s.l. (Fig. 9). Similarly, AAR_0 was

486   computed as ~54% for steady-state glacier–wide MB.
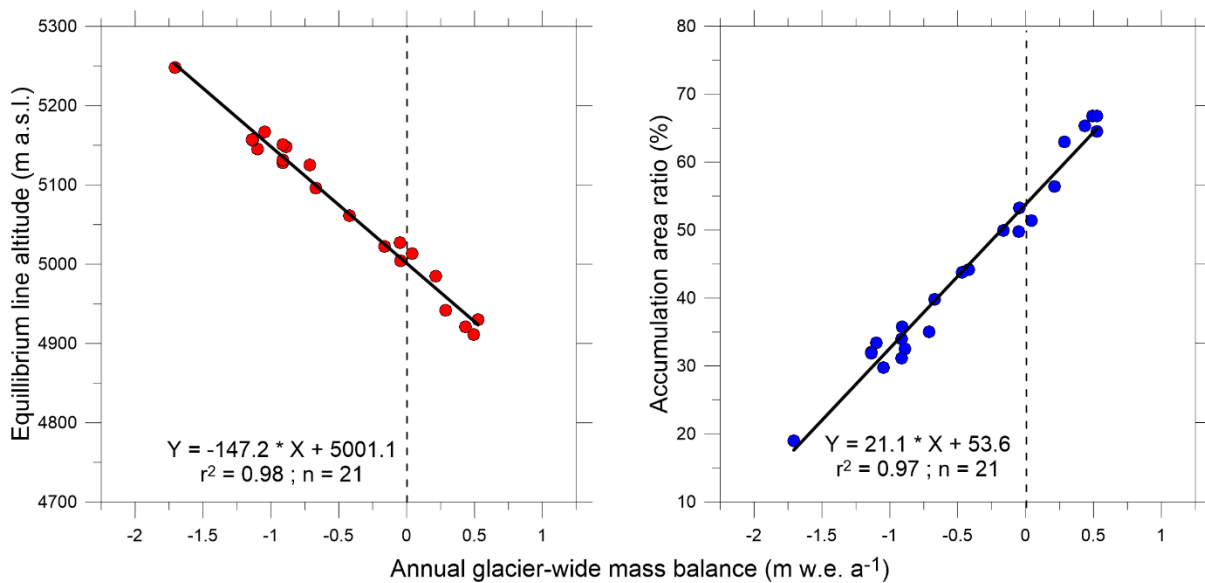
Figure 9: The ELA and AAR as a function of annual glacier–wide MB.

5. Discussion

5.1 Biases in glacier–wide mass balances and performance of nonlinear model

A total of 358 annual ablation and 65 annual accumulation point measurements were collected on Chhota Shigri Glacier over 2002–2023 to estimate the glacier–wide MBs (five ablation and five accumulation point MB measurements were removed before final model run; section 3.3). Figure 10 shows the temporal evolution of the number of these point measurements, and Table S1 provides the details about these point MBs. In general, the point MB measurement network (especially the accumulation points) has been poor after 2014 (section 3.1, Fig. 10). The eastern accumulation site at 5550 m a.s.l. (Fig. 1) could only be accessed five times (2003, 2004, 2005, 2009, 2011) over the 2002-2023 period, while no accumulation measurements were done in 2018, 2020 and 2021 (section 3.1). Occasionally, the ablation measurements were also missing due to missing stakes (heavy ablation or destroyed stakes). In the traditional method, these missing measurements were filled with extrapolated values from nearby ablation/accumulation MB measurements or previous years' point MB measurements to estimate the glacier–wide MBs (Azam et al., 2016; Mandal et al., 2020; Table S1).
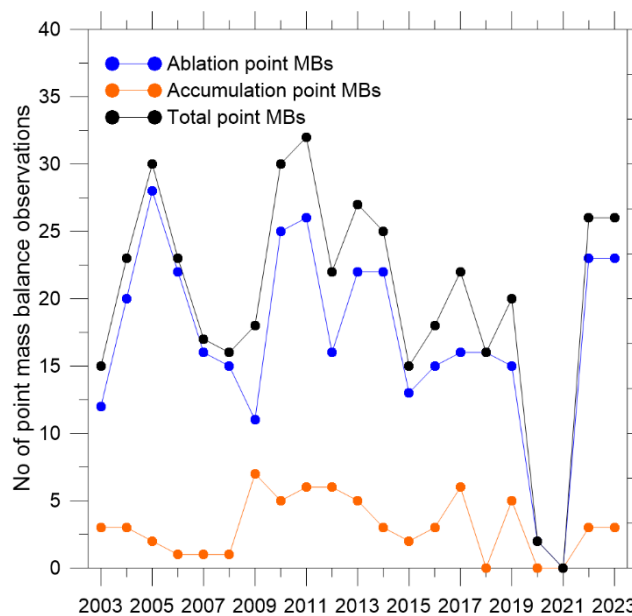
Figure 10: Number of available ablation, accumulation, and total point MBs for each hydrological year between 2002 and 2023.

The systematic biases in glacier–wide annual MB series with the same monitoring network are expected to be of the same sign throughout the observation period, and the series is systematically adjusted to match the geodetic MBs available over one or more periods (Zemp et al., 2013; Wagnon et al., 2021). Nonlinear MB series on Chhota Shigri Glacier

showed negative biases (–0.03 and –0.17 m w.e. a^{-1} over the 2003-2014 and 2014-2020 periods, respectively), suggesting that the nonlinear model can reasonably estimate the glacier–wide MBs with the existing monitoring network. Conversely, the traditional MB series showed a negative bias (–0.10 m w.e. a^{-1}) over the 2003-2014 period and a large, positive bias (0.33 m w.e. a^{-1}) over the 2014-2020 (Fig. 8; Table 2). The major disagreement between the cumulative nonlinear and traditional MB curves after 2017 (Fig. 8) is likely due to a degradation of the quality of field observations due to harsh weather, too short field surveys, or observers not being sufficiently experienced (Fig. 10; Table S1; section 3.1). Wagnon et al. (2021) performed a thorough analysis on Mera Glacier (Dush Koshi Basin, Nepal) and identified the precise source of systematic bias in the glacier–wide MB by comparing the surface-specific mass balance calculated using the traditional glaciological method of a specific zone on the glacier with that derived from the ice-flux method (based on the mass conservation equation). Unfortunately, we could not conduct such an analysis in the current study due to insufficient data availability. However, future research will include this comparative analysis to uncover any systematic biases in the glacier-wide MB data series for the Chhota Shigri Glacier.

To further investigate the performance of the nonlinear model compared to the traditional MB method, we calibrated both the MB series with the geodetic MB estimated using ASTER (08/10/2003) and Pléiades (12/09/2020) DEMs (details in SI) and used the geodetic MB over 2003–2014 (section 4.2) to validate both the calibrated series. The calibrated nonlinear MB series showed a good agreement with the available geodetic MB (–3.88 m w.e. against –4.18 m w.e.), while the traditional MB showed very strong deviation from the geodetic MB over 2003–2014 (–6.13 m w.e. against –4.18 m w.e.) (Fig. S1). This good agreement between nonlinear and geodetic MBs over 2003-2014 shows the robustness of the nonlinear model for the glacier–wide mass balance estimation. Further, this comparison also highlights the importance of using short-duration geodetic MB estimates for the calibration process, as with two calibration periods, the calibrated traditional MB is in better agreement with the geodetic MB (Fig. S1).

The nonlinear model shows a much better agreement with geodetic MBs than the traditional method (Fig. 8; Table 2) mainly due to the (i) capability of the nonlinear model to better capture the spatial variability of surface MB from a heterogeneous, discontinuous and limited point MB data series than the traditional method (Vincent et al., 2018), (ii) correction/exclusion of erroneous measurements (section 3.3) and (iii) exclusion of the extrapolated ablation/accumulation points in the nonlinear model that might have introduced

547   biases in traditional MB (Fig. S2). The extrapolated point-MBs in the accumulation area

548   showed a difference ranging from −1.98 to 1.74 m w.e. between modelled and extrapolated,

549   especially post-2014 (Fig. S2 and S3). The better performance of the nonlinear model

550   suggests that the extrapolation of point accumulations (in case of missing point

551   measurements) in estimating the glacier–wide MB using the traditional method is risky.

5.2 2019/20 glacier–wide mass balance from two point mass balances

553   The spatial and temporal terms in equation (2) are computed from a data sample available

554   from the whole series; therefore, MB computation is expected to be affected by missing data

555   from any single year (or, in general, from all years whenever data is missing). The

556   glacier–wide MB for 2019/20 was estimated using only two point MB observations (section

557   3.2; Table S1); therefore, it might have biases (Lliboutry, 1974; Vincent et al., 2018).

558   To investigate the additional error, we selected the year 2022/23 to test the

559   performance of the nonlinear model. The 2022/23 year was selected because it is among the

560   years with the maximum of point MB observations, and they were performed at their original

561   locations. The nonlinear model was re-run over the 2002-2023 period, keeping only two point

562   MB data (out of 26) for 2022/23 year corresponding to the locations of the two point MB

563   measurements in 2019/20. With only two point MBs, the glacier–wide MB for 2022/23 was

564   recomputed to be 0.13 m w.e. a^{-1} against the original MB of 0.04 m w.e. a^{-1} with a difference

565   of 0.09 m w.e. a^{-1}, while all other year's glacier–wide MBs were changed by a maximum of

566   ±0.01 m w.e. a^{-1} (Fig. 11A). As expected, the changes in the temporal term, β_t, having a

567   glacier–wide significance, showed significant deviation from 0.93 to 1.06 m w.e. a^{-1} for

568   2022/23 year, while for other years it changed by maximum up to ±0.04 m w.e. a^{-1} (Fig.

569   11B). Conversely, the deviations in mean altitudinal spatial terms α_e and γ_e were very small

570   (maximum up to ±0.06 m w.e. and ±0.005, respectively) (Fig. 11C, 11D). Therefore, the

571   temporal term (β_t) in equation (2) mainly controls the annual glacier–wide MB.
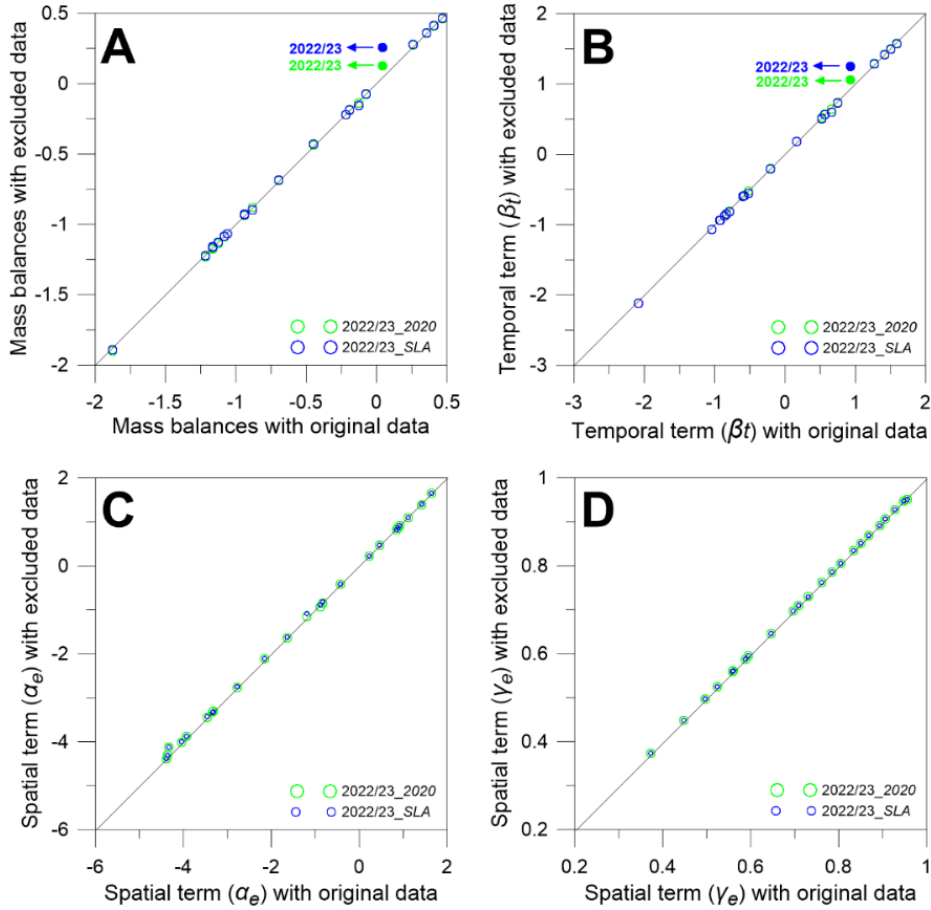
Figure 11: Glacier–wide MBs (**A**), temporal (β_t) (**B**) and spatial terms (α_e, and γ_e) (**C and D, respectively**) obtained with the nonlinear model following two different scenarios as a function of their original values obtained with the full dataset. In the first scenario (2022/23_*2020*), we remove all the data from 2022/23 (24-point MBs) except two located at the observation points in 2019/20 (see section 5.2). In the second scenario (2022/23_*SLA*), we remove all the data from 2022/23 and keep only two point MB data (= 0 m w.e.) obtained along the SLA (see section 5.3). The filled dots highlight the test year of 2022/23.

The deviation of 0.09 m w.e. a^{-1} in glacier–wide MB estimated with only two point MBs is less than the estimated random error of 0.27 m w.e. a^{-1} in the 2022/23 glacier–wide MB in the original model run; therefore, it is assumed that the error in 2019/20 glacier–wide MB due to restricted number of MB measurements is also less than the estimated random error of 0.16 m w.e. a^{-1} (Table 3). Unlike the traditional MB method, the nonlinear model can fill the gaps in glacier–wide MB where some point MB observations are missing and can provide a consistent series of temporal fluctuations.

5.3 2020/21 glacier–wide mass balance from nonlinear model-SLA method

The glacier–wide MB for 2020/21 year was estimated by inferring two point MB input from end-of-summer SLA, assuming it to be equivalent to ELA (i.e., MB = 0 m w.e.) (section 3.2;

Fig. 3). Due to only two point MB input data, the modelled glacier–wide MB for 2020/21 may also have additional errors.

To quantify this error, we repeated the same exercise as in section 5.2 for the year 2022/23, this time keeping again two point MB data of 2022/23, but at the two sites where point MB data have been assessed to be zero in 2020/21. The resulting 2022/23 glacier-wide MB is 0.26 m w.e. a^{-1}, 0.22 m w.e. a^{-1} higher than the original value (Fig. 11A), mainly explained by the β_t term (Fig. 11B). This difference is still lower than the estimated random error of 0.27 m w.e. a^{-1} in 2022/23 (Table 3). However, there are still possible biases in glacier–wide MB of 2020/21 year as the SLA was delineated from a Sentinel image from 6 September 2021 (section 3.2; Fig. 3) that is not exactly from the end of ablation season (30 September) on Chhota Shigri Glacier. The surface energy balance model estimated a MB of –0.19 m w.e. over the 6 September – 30 September 2021 (Srivastava and Azam, 2022a). However, this seasonal offset correction in SLA-derived annual MB may be given, but it was avoided as the differences are within the estimated random error of 0.20 m w.e. a^{-1} (Table 3). Our analysis shows that the glacier-wide MB can also be estimated from SLA using the nonlinear model if the field measurements cannot be carried out for some specific years.

However, the nonlinear model-SLA method has several limitations: (i) the delineated SLA must pass through grid/s having previous point MB observation/s (Fig. 3) as at least one previous measurement is required to run the model, (ii) the delineated SLA must be from the end of ablation season to consider it as ELA, (iii) SLA delineation has its challenges and often it is difficult to find the cloud-free image for delineation at the end of ablation season (Brun et al., 2015; Racoviteanu et al., 2019), and (iv) SLA is severely affected by recent snowfall hence must be checked with in-situ precipitation data before using SLA in nonlinear model. This latter point implies that the ELA can be inferred from the end-of-ablation-season SLA, which is not always possible over glaciers, especially in monsoon-dominated regions (Brun et al., 2015).

5.4 Recommendation: apply the nonlinear model on other glaciers

This study demonstrates that the nonlinear model outperforms the traditional method for estimating glacier-wide MB (section 5.1). Apart from the present research, the nonlinear model has been applied only to the Mera Glacier in the Himalaya (Wagnon et al., 2021) and on Argentière, Saint Sorlin, Mer de Glace, and Gébroulaz (France, Alps), Zongo (Bolivia, Andes), and Nigardsbreen (Norway, Scandinavia) glaciers (Vincent et al., 2018).

Equation (1) includes a spatial effect term (γ_i) that accounts for the standard deviations in point MBs across elevation. This term typically requires around ten years of point MB observations to be accurately estimated (Vincent et al., 2018). Therefore, applying the nonlinear model wherever MB observations are available for around ten years is advisable, especially in the Himalaya where data accessibility issues often lead to gaps in observations (Azam et al., 2018). We recommend extending the application of the nonlinear model to other Himalayan glaciers that have consistent MB observations spanning approximately ten years, such as Kolahoi, Hoksar and Sutri Dhaka glaciers in the western Himalaya, and Chorabari, Dokriani Bamak, Pokalde, Rikha Samba, Yala, West Changri Nup glaciers in the central Himalaya, etc. However, the estimated glacier-wide MBs may contain systematic biases due to the distribution of point measurements across the glacier. Therefore, they should be verified and, if necessary, reanalyzed using geodetic estimates.

Conclusions

This work reanalyses glacier–wide MBs by combining the traditional reanalysis framework (Zemp et al., 2013) and the nonlinear MB model (Vincent et al., 2018). Previously, the annual glacier–wide MBs had been estimated on Chhota Shigri Glacier since 2002, when the traditional glaciological method was applied using heterogeneous in-situ point MB measurements. The heterogeneous measurement network does not always catch the large spatiotemporal variability of point MBs; hence, the point MB-elevation relationship is insufficient to investigate the changes in glacier–wide MBs. Therefore, we applied the nonlinear model to compute the glacier–wide MBs of Chhota Shigri Glacier as it enables the computation of the glacier–wide MB from a heterogeneous in-situ point MB network. The nonlinear model was used to detect the measurement errors. Five of the 423-point measurements were corrected from field notebooks, and ten were recognized as wrong observations and discarded before running the final model.

ASTER and Pléiades DEMs were used to estimate the geodetic MBs over 2003–2014 and 2014–2020 and they have been used to reanalyse the nonlinear MBs. Nonlinear MBs agreed well with the geodetic estimates available over 2003–2014 and 2014–2020, unlike traditional MBs that showed large differences, especially over the 2014–2020 period. The reanalysed nonlinear MBs showed a large annual variability ranging from 0.53 ± 0.16 m w.e. a^{-1} in 2018/19 to -1.71 ± 0.24 m w.e. a^{-1} in 2021/22. The Chhota Shigri Glacier is imbalanced with a mean mass wastage of -0.47 ± 0.19 m w.e. a^{-1}, equivalent to a cumulative loss of -9.81 ± 0.87 m w.e. over 2002–2023.

With the 21-year-long MB observations, the Chhota Shigri Glacier MB series is the longest in the Himalaya. This work has enabled the data set to be extended, optimised, and corrected to provide the best possible mass balance series for this benchmark glacier. We plan to monitor this glacier over a long period, with repeated satellite image acquisitions by the Pléiades Glacier Observatory to regularly validate/calibrate the glacier–wide MB, typically every five years.

Our detailed analysis suggests that the nonlinear model performs better in calculating the glacier–wide MB than the traditional method as (i) the nonlinear MBs are in much better agreement with the geodetic MB estimates, (ii) it can detect erroneous measurements, (iii) it provides better glacier–wide MBs than those of the traditional method when the observational network is very limited, and (iv) glacier–wide MB can be computed using SLA if the ablation-end SLA passes through a grid cell that contains point MB observations from previous years. Therefore, the application of the nonlinear model is suggested on all monitored glaciers whenever data is sufficient. It becomes even more relevant in the Himalaya, where data are sometimes missing due to access issues. However, the estimated glacier–wide MBs may contain systematic bias (arises from the distribution of point measurements over the glacier) and, therefore, should be checked and, if necessary, reanalysed with geodetic estimates.

Author contribution

MFA, CV and PW conceptualised the study. MFA did the nonlinear model runs and analysed the data with the help of CV and PW. SS estimated the areal changes, the snow line altitudes, and MBs from the energy balance model. EB estimated the geodetic MBs. MFA wrote the paper with inputs from all co-authors.

Competing interests

At least one of the (co-)authors is a member of the editorial board of The Cryosphere.

Acknowledgements

MFA acknowledges the research grants from ISRO under the RESPOND scheme (ISRO/RES/4/690/21-22), SERB (CRG/2020/004877) and MoES (MOES/PAMC/H&C/131/2019-PC-II). EB acknowledges support from the French Space Agency (CNES). Pléiades stereo-imagery of September 2020 was obtained through the Pléiades Glacier Observatory. The authors are grateful to DST-IFCPAR/CEFIPRA project n°3900-W1 and the French Service d'Observation GLACIOCLIM sponsored by IRD, which

provided financial support to conduct field trips and equipment. Thanks to all scientists, Adhikari Ji and porters involved in the previous research expeditions on Chhota Shigri Glacier since 2002.

Code/Data Availability

Detailed model documentation, tutorial and model codes can be found on the website of the GLACIOCLIM program (https://glacioclim.osug.fr). The data used in this study can be requested from the corresponding author.

References

Andreassen, L. M., Elvehøy, H., Kjøllmoen, B., and Engeset, R. V.: Reanalysis of long-term series of glaciological and geodetic mass balance for 10 Norwegian glaciers, The Cryosphere, 10, 535–552, https://doi.org/10.5194/tc-10-535-2016, 2016.

Andreassen, L. M., Nagy, T., Kjøllmoen, B., and Leigh, J. R.: An inventory of Norway's glaciers and ice-marginal lakes from 2018–19 Sentinel-2 data, Journal of Glaciology, 68, 1085–1106, https://doi.org/10.1017/jog.2022.20, 2022.

Azam, M. F.: Need of integrated monitoring on reference glacier catchments for future water security in Himalaya, Water Security, 14, 100098, https://doi.org/10.1016/j.wasec.2021.100098, 2021.

Azam, M. F., Wagnon, P., Ramanathan, A., Vincent, C., Sharma, P., Arnaud, Y., Linda, A., Pottakkal, J. G., Chevallier, P., Singh, V. B., and Berthier, E.: From balance to imbalance: a shift in the dynamic behaviour of Chhota Shigri glacier, western Himalaya, India, Journal of Glaciology, 58, 315–324, https://doi.org/10.3189/2012JoG11J123, 2012.

Azam, M. F., Wagnon, P., Vincent, C., Ramanathan, A., Linda, A., and Singh, V. B.: Reconstruction of the annual mass balance of Chhota Shigri glacier, Western Himalaya, India, since 1969, Annals of Glaciology, 55, 69–80, https://doi.org/10.3189/2014AoG66A104, 2014.

Azam, M. F., Ramanathan, A., Wagnon, P., Vincent, C., Linda, A., Berthier, E., Sharma, P., Mandal, A., Angchuk, T., Singh, V. B., and Pottakkal, J. G.: Meteorological conditions, seasonal and annual mass balances of Chhota Shigri Glacier, western Himalaya, India, Annals of Glaciology, 57, 328–338, https://doi.org/10.3189/2016AoG71A570, 2016.

Azam, M. F., Wagnon, P., Berthier, E., Vincent, C., Fujita, K., and Kargel, J. S.: Review of the status and mass changes of Himalayan-Karakoram glaciers, Journal of Glaciology, 64, 61–74, https://doi.org/10.1017/jog.2017.86, 2018.

Azam, M. F., Kargel, J. S., Shea, J. M., Nepal, S., Haritashya, U. K., Srivastava, S., Maussion, F., Qazi, N., Chevallier, P., Dimri, A. P., Kulkarni, A. V., Cogley, J. G., and Bahuguna, I.: Glaciohydrology of the Himalaya-Karakoram, Science, 373, eabf3668, https://doi.org/10.1126/science.abf3668, 2021.

Banerjee, A. and Shankar, R.: On the response of Himalayan glaciers to climate change, Journal of Glaciology, 59, 480–490, https://doi.org/10.3189/2013JoG12J130, 2013.

Barandun, M., Pohl, E., Naegeli, K., McNabb, R., Huss, M., Berthier, E., Saks, T., and Hoelzle, M.: Hot Spots of Glacier Mass Balance Variability in Central Asia, Geophysical Research Letters, 48, e2020GL092084, https://doi.org/10.1029/2020GL092084, 2021.

Basantes-Serrano, R., Rabatel, A., Francou, B., Vincent, C., Maisincho, L., Cáceres, B., Galarraga, R., and Alvarez, D.: Slight mass loss revealed by reanalyzing glacier mass-balance observations on Glacier Antisana 15α (inner tropics) during the 1995–2012 period, Journal of Glaciology, 62, 124–136, https://doi.org/10.1017/jog.2016.17, 2016.

Berthier, E., Arnaud, Y., Kumar, R., Ahmad, S., Wagnon, P., and Chevallier, P.: Remote sensing estimates of glacier mass balances in the Himachal Pradesh (Western Himalaya, India), Remote Sensing of Environment, 108, 327–338, https://doi.org/10.1016/j.rse.2006.11.017, 2007.

Berthier, E., Floricioiu, D., Gardner, A. S., Gourmelen, N., Jakob, L., Paul, F., Treichler, D., Wouters, B., Belart, J. M. C., Dehecq, A., Dussaillant, I., Hugonnet, R., Kaab, A. M., Krieger, L., Pálsson, F., and Zemp, M.: Measuring Glacier Mass Changes from Space - A Review, Reports on Progress in Physics, 86, 036801, https://doi.org/10.1088/1361-6633/acaf8e, 2023.

Bolch, T., Yao, T., Kang, S., Buchroithner, M. F., Scherer, D., Maussion, F., Huintjes, E., and Schneider, C.: A glacier inventory for the western Nyainqentanglha Range and the Nam Co Basin, Tibet, and glacier changes 1976–2009, The Cryosphere, 4, 419–433, https://doi.org/10.5194/tc-4-419-2010, 2010.

746 Bolch, T., Shea, J. M., Liu, S., Azam, F. M., Gao, Y., Gruber, S., Immerzeel, W. W.,

747 Kulkarni, A., Li, H., Tahir, A. A., Zhang, G., and Zhang, Y.: Status and Change of the

748 Cryosphere in the Extended Hindu Kush Himalaya Region, in: The Hindu Kush Himalaya

749 Assessment: Mountains, Climate Change, Sustainability and People, edited by: Wester, P.,

750 Mishra, A., Mukherji, A., and Shrestha, A. B., Springer International Publishing, Cham, 209–

751 255, https://doi.org/10.1007/978-3-319-92288-1_7, 2019.

752 Brun, F., Berthier, E., Wagnon, P., Kääb, A., and Treichler, D.: A spatially resolved estimate

753 of High Mountain Asia glacier mass balances from 2000 to 2016, Nature Geosci, 10, 668–

754 673, https://doi.org/10.1038/ngeo2999, 2017.

755 Brun, F., Dumont, M., Wagnon, P., Berthier, E., Azam, M. F., Shea, J. M., Sirguey, P.,

756 Rabatel, A., and Ramanathan, Al.: Seasonal changes in surface albedo of Himalayan glaciers

757 from MODIS data and links with the annual mass balance, The Cryosphere, 9, 341–355,

758 https://doi.org/10.5194/tc-9-341-2015, 2015.

759 Chand, P. and Sharma, M. C.: Frontal changes in the Manimahesh and Tal Glaciers in the

760 Ravi basin, Himachal Pradesh, northwestern Himalaya (India), between 1971 and 2013,

761 International Journal of Remote Sensing, 36, 4095–4113,

762 https://doi.org/10.1080/01431161.2015.1074300, 2015.

763 Cogley, J., Hock, R., Rasmussen, L., Arendt, A., Bauder, A., Braithwaite, R., Jansson, P.,

764 Kaser, G., Möller, M., Nicholson, L., and Zemp, M.: Glossary of glacier mass balance and

765 related terms, https://doi.org/10.5167/uzh-53475, 2011.

766 Cogley, J. G.: Geodetic and direct mass-balance measurements: comparison and joint

767 analysis, Annals of Glaciology, 50, 96–100, https://doi.org/10.3189/172756409787769744,

768 2009.

769 Cuffey, K. M. and Paterson, W. S. B.: The Physics of Glaciers, Academic Press, 721 pp.,

770 2010.

771 Davaze, L., Rabatel, A., Dufour, A., Hugonnet, R., and Arnaud, Y.: Region-wide annual

772 glacier surface mass balance for the European Alps from 2000 to 2016, Frontiers in Earth

773 Science, 8, 149, https://doi.org/10.3389/feart.2020.00149, 2020.

774 Falaschi, D., Bhattacharya, A., Guillet, G., Huang, L., King, O., Mukherjee, K., Rastner, P.,

775 Yao, T., and Bolch, T.: Annual to seasonal glacier mass balance in High Mountain Asia

derived from Pléiades stereo images: examples from the Pamir and the Tibetan Plateau, The Cryosphere, 17, 5435–5458, https://doi.org/10.5194/tc-17-5435-2023, 2023.

Funk, M., Morelli, R., and Stahel, W.: Mass balance of Griesgletscher 1961-1994: Different methods of determination, Massenbilanz des Griesgletschers 1961-1994: Verschiedene Bestimmungsverfahren, 33, 41–56, 1997.

Gantayat, P. and Ramsankaran, R.: Modelling evolution of a large, glacier-fed lake in the Western Indian Himalaya, Sci Rep, 13, 1840, https://doi.org/10.1038/s41598-023-28144-8, 2023.

Gardner, A., Moholdt, G., Cogley, J., Wouters, B., Arendt, A., Wahr, J., Berthier, E., Hock, R., Pfeffer, W., Kaser, G., Ligtenberg, S., Bolch, T., Sharp, M., Hagen, J., Van den Broeke, M., and Paul, F.: A Reconciled Estimate of Glacier Contributions to Sea Level Rise: 2003 to 2009, Science (New York, N.Y.), 340, 852–857, https://doi.org/10.1126/science.1234532, 2013.

Garg, P. K., Shukla, A., and Jasrotia, A. S.: Influence of topography on glacier changes in the central Himalaya, India, Global and Planetary Change, 155, 196–212, https://doi.org/10.1016/j.gloplacha.2017.07.007, 2017.

Haq, M. A., Azam, M.F., Vincent, C.: Efficiency of artificial neural networks for glacier ice-thickness estimation: a case study in western Himalaya, India. Journal of Glaciology 67(264), 671–684, https://doi.org/10.1017/jog.2021.19, 2021.

Harrison, S., Kargel, J. S., Huggel, C., Reynolds, J., Shugar, D. H., Betts, R. A., Emmer, A., Glasser, N., Haritashya, U. K., Klimeš, J., Reinhardt, L., Schaub, Y., Wiltshire, A., Regmi, D., and Vilímek, V.: Climate change and the global pattern of moraine-dammed glacial lake outburst floods, The Cryosphere, 12, 1195–1209, https://doi.org/10.5194/tc-12-1195-2018, 2018.

Hugonnet, R., McNabb, R., Berthier, E., Menounos, B., Nuth, C., Girod, L., Farinotti, D., Huss, M., Dussaillant, I., Brun, F., and Kääb, A.: Accelerated global glacier mass loss in the early twenty-first century, Nature, 592, 726–731, https://doi.org/10.1038/s41586-021-03436-z, 2021.

Huss, M., Bauder, A., and Funk, M.: Homogenization of long-term mass-balance time series, Annals of Glaciology, 50, 198–206, https://doi.org/10.3189/172756409787769627, 2009.

Jackson, M., Azam, M. F., Baral, P., Benestad, R., Brun, F., Muhammad, S., Pradhananga, S., Shrestha, F., Steiner, J. F., and Thapa, A.: Chapter 2: Consequences of climate change for the cryosphere in the Hindu Kush Himalaya, https://doi.org/10.53055/ICIMOD.1030, 2023.

Kuhn, M.: Mass Budget Imbalances as Criterion for a Climatic Classification of Glaciers, Geografiska Annaler. Series A, Physical Geography, 66, 229–238, https://doi.org/10.2307/520696, 1984.

Kumar, A., Verma, A., Gokhale, A., Bhambri, R., Misra, A., Sundriyal, S., Dobhal, D., and kishore, N.: Hydrometeorological assessments and suspended sediment delivery from a central Himalayan glacier in the upper Ganga basin, International Journal of Sediment Research, 33, https://doi.org/10.1016/j.ijsrc.2018.03.004, 2018.

Laha, S., Kumari, R., Singh, S., Mishra, A., Sharma, T., Banerjee, A., Nainwal, H. C., and Shankar, R.: Evaluating the contribution of avalanching to the mass balance of Himalayan glaciers, Annals of Glaciology, 58, 110–118, https://doi.org/10.1017/aog.2017.27, 2017.

Lliboutry, L.: Multivariate Statistical Analysis of Glacier Annual Balances, Journal of Glaciology, 13, 371–392, https://doi.org/10.3189/S0022143000023169, 1974.

Mandal, A., Ramanathan, A., Azam, M. F., Angchuk, T., Soheb, M., Kumar, N., Pottakkal, J. G., Vatsal, S., Mishra, S., and Singh, V. B.: Understanding the interrelationships among mass balance, meteorology, discharge and surface velocity on Chhota Shigri Glacier over 2002–2019 using in situ measurements, Journal of Glaciology, 66, 727–741, https://doi.org/10.1017/jog.2020.42, 2020.

Mandal, A., Angchuk, T., Azam, M. F., Ramanathan, A., Wagnon, P., Soheb, M., and Singh, C.: An 11-year record of wintertime snow-surface energy balance and sublimation at 4863 m a.s.l. on the Chhota Shigri Glacier moraine (western Himalaya, India), The Cryosphere, 16, 3775–3799, https://doi.org/10.5194/tc-16-3775-2022, 2022.

Miles, E., McCarthy, M., Dehecq, A., Kneib, M., Fugger, S., and Pellicciotti, F.: Health and sustainability of glaciers in High Mountain Asia, Nat Commun, 12, 2868, https://doi.org/10.1038/s41467-021-23073-4, 2021.

Mukherjee, K., Bhattacharya, A., Pieczonka, T., Ghosh, S., and Bolch, T.: Glacier mass budget and climate reanalysis data indicate a climatic shift around 2000 in Lahaul-Spiti,

western Himalaya, Climatic Change, 148, 219–233, https://doi.org/10.1007/s10584-018-2185-3, 2018.

Nepal, S., Steiner, J. F., Allen, S., Azam, M. F., Bhuchar, S., Biemans, H., Dhakal, M., Khanal, S., Li, D., Lutz, A., Pradhananga, S., Ritzema, R., Stoffel, M., and Stuart-Smith, R.: Chapter 3: Consequences of cryospheric change for water resources and hazards in the Hindu Kush Himalaya, https://doi.org/10.53055/ICIMOD.1031, 2023.

Oerlemans, J.: Glaciers and Climate Change, CRC Press, 168 pp., 2001.

Østrem, G. and Stanley, A.: Glacier mass balance measurements: a manual for field and office work. 1969.

Østrem, G. and Brugman, M.: Glacier mass-balance measurements: a manual for field and office work, 1991.

Oulkar, S. N., Thamban, M., Sharma, P., Pratap, B., Singh, A. T., Patel, L. K., Pramanik, A. and Ravichandran, M.: Energy fluxes, mass balance, and climate sensitivity of the Sutri Dhaka Glacier in the western Himalaya. Front. Earth Sci. 10:949735. doi:10.3389/feart.2022.949735 , 2022.

Rabatel, A., Dedieu, J.-P., and Vincent, C.: Using remote-sensing data to determine equilibrium-line altitude and mass-balance time series: validation on three French glaciers, 1994–2002, Journal of Glaciology, 51, 539–546, https://doi.org/10.3189/172756505781829106, 2005.

Racoviteanu, A. E., Rittger, K., and Armstrong, R.: An automated approach for estimating snowline altitudes in the Karakoram and eastern Himalaya from remote sensing, Frontiers in Earth Science, 7, 220, https://doi.org/10.3389/feart.2019.00220, 2019.

Ramsankaran, R., Pandit, A., and Azam, M. F.: Spatially distributed ice-thickness modelling for Chhota Shigri Glacier in western Himalayas, India, International Journal of Remote Sensing, 39, 3320–3343, https://doi.org/10.1080/01431161.2018.1441563, 2018.

Raup, B., Racoviteanu, A., Khalsa, S. J. S., Helm, C., Armstrong, R., and Arnaud, Y.: The GLIMS geospatial glacier database: A new tool for studying glacier change, Global and Planetary Change, 56, 101–110, https://doi.org/10.1016/j.gloplacha.2006.07.018, 2007.

Romshoo, S. A., Murtaza, K. O. & Abdullah, T.: Towards understanding various influences on mass balance of the Hoksar Glacier in the Upper Indus Basin using observations. Sci Rep **12**, 15669. https://doi.org/10.1038/s41598-022-20033-w, 2022.

Romshoo, S. A., Abdullah, T., Murtaza, K. O., Bhat, M. H.: Direct, geodetic and simulated mass balance studies of the Kolahoi Glacier in the Kashmir Himalaya. India, Journal of Hydrology, 617:129019. https://doi.org/ 10.1016/j.jhydrol.2022.129019, 2023.

Rounce, D. R., Hock, R., Maussion, F., Hugonnet, R., Kochtitzky, W., Huss, M., Berthier, E., Brinkerhoff, D., Compagno, L., Copland, L., Farinotti, D., Menounos, B., and McNabb, R. W.: Global glacier change in the 21st century: Every increase in temperature matters, Science, 379, 78–83, https://doi.org/10.1126/science.abo1324, 2023.

Shean, D. E., Bhushan, S., Montesano, P., Rounce, D. R., Arendt, A., and Osmanoglu, B.: A Systematic, Regional Assessment of High Mountain Asia Glacier Mass Balance, Frontiers in Earth Science, 7, https://doi.org/10.3389/feart.2019.00363, 2020.

Shugar, D. H., Jacquemart, M., Shean, D., Bhushan, S., Upadhyay, K., Sattar, A., Schwanghart, W., McBride, S., De Vries, M. V. W., Mergili, M., Emmer, A., Deschamps-Berger, C., McDonnell, M., Bhambri, R., Allen, S., Berthier, E., Carrivick, J. L., Clague, J. J., Dokukin, M., Dunning, S. A., Frey, H., Gascoin, S., Haritashya, U. K., Huggel, C., Kääb, A., Kargel, J. S., Kavanaugh, J. L., Lacroix, P., Petley, D., Rupper, S., Azam, M. F., Cook, S. J., Dimri, A. P., Eriksson, M., Farinotti, D., Fiddes, J., Gnyawali, K. R., Harrison, S., Jha, M., Koppes, M., Kumar, A., Leinss, S., Majeed, U., Mal, S., Muhuri, A., Noetzli, J., Paul, F., Rashid, I., Sain, K., Steiner, J., Ugalde, F., Watson, C. S., and Westoby, M. J.: A massive rock and ice avalanche caused the 2021 disaster at Chamoli, Indian Himalaya, Science, 373, 300–306, https://doi.org/10.1126/science.abh4455, 2021.

Shukla, A. and Qadir, J.: Differential response of glaciers with varying debris cover extent: evidence from changing glacier parameters, International Journal of Remote Sensing, 37, 2453–2479, https://doi.org/10.1080/01431161.2016.1176272, 2016.

Shukla, A., Garg, P. K., and Srivastava, S.: Evolution of Glacial and High-Altitude Lakes in the Sikkim, Eastern Himalaya Over the Past Four Decades (1975–2017), Front. Environ. Sci., 6, 81, https://doi.org/10.3389/fenvs.2018.00081, 2018.

Soruco, A., Vincent, C., Francou, B., Ribstein, P., Berger, T., Sicart, J. E., Wagnon, P., Arnaud, Y., Favier, V., and Lejeune, Y.: Mass Balance of Glaciar Zongo, Bolivia, between

1956 and 2006, using glaciological, hydrological and geodetic methods, Annals of Glaciology, 50, 1–8, https://doi.org/10.3189/172756409787769799, 2009.

Srivastava, S. and Azam, M. F.: Mass- and Energy-Balance Modeling and Sublimation Losses on Dokriani Bamak and Chhota Shigri Glaciers in Himalaya Since 1979, Frontiers in Water, 4, 874240, https://doi.org/10.3389/frwa.2022.874240, 2022a.

Srivastava, S. and Azam, Mohd. F.: Functioning of glacierized catchments in Monsoon and Alpine regimes of Himalaya, Journal of Hydrology, 609, 127671, https://doi.org/10.1016/j.jhydrol.2022.127671, 2022b.

Srivastava, S., Garg, P. K., and Azam, Mohd. F.: Seven Decades of Dimensional and Mass Balance Changes on Dokriani Bamak and Chhota Shigri Glaciers, Indian Himalaya, Using Satellite Data and Modelling, J Indian Soc Remote Sens, 50, 37–54, https://doi.org/10.1007/s12524-021-01455-x, 2022.

Stokes, C. R., Clark, C. D., Lian, O. B., and Tulaczyk, S.: Ice stream sticky spots: A review of their identification and influence beneath contemporary and palaeo-ice streams, Earth-Science Reviews, 81, 217–249, https://doi.org/10.1016/j.earscirev.2007.01.002, 2007.

Stumm, D., Joshi, S. P., Gurung, T. R., and Silwal, G.: Mass balances of Yala and Rikha Samba glaciers, Nepal, from 2000 to 2017. Earth System Science Data, 13(8), 3791–3818. doi:10.5194/essd-13-3791-2021, 2021.

Sunako, S., Fujita, K., Sakai, A., and Kayastha, R.: Mass balance of Trambau Glacier, Rolwaling region, Nepal Himalaya: In-situ observations, long-term reconstruction and mass-balance sensitivity, Journal of Glaciology 65, 605–616. doi:10.1017/jog.2019.37, 2019.

Tshering, P. and Fujita, K.: First in situ record of decadal glacier mass balance (2003–2014) from the Bhutan Himalaya. Annals of Glaciology, 57(71), 289-294, doi:10.3189/2016AoG71A036, 2016.

Thibert, E., Blanc, R., Vincent, C., and Eckert, N.: Glaciological and volumetric mass-balance measurements: error analysis over 51 years for Glacier de Sarennes, French Alps, Journal of Glaciology, 54, 522–532, https://doi.org/10.3189/002214308785837093, 2008.

Vincent, C., Ramanathan, A., Wagnon, P., Dobhal, D. P., Linda, A., Berthier, E., Sharma, P., Arnaud, Y., Azam, M. F., Jose, P. G., and Gardelle, J.: Balanced conditions or slight mass gain of glaciers in the Lahaul and Spiti region (northern India, Himalaya) during the nineties

924 preceded recent mass loss, The Cryosphere, 7, 569–582, https://doi.org/10.5194/tc-7-569-
925 2013, 2013.

926 Vincent, C., Soruco, A., Azam, M. F., Basantes-Serrano, R., Jackson, M., Kjøllmoen, B.,
927 Thibert, E., Wagnon, P., Six, D., Rabatel, A., Ramanathan, A., Berthier, E., Cusicanqui, D.,
928 Vincent, P., and Mandal, A.: A Nonlinear Statistical Model for Extracting a Climatic Signal
929 From Glacier Mass Balance Measurements, Journal of Geophysical Research: Earth Surface,
930 123, 2228–2242, https://doi.org/10.1029/2018JF004702, 2018.

931 Vishwakarma, B. D., Ramsankaran, R., Azam, M. F., Bolch, T., Mandal, A., Srivastava, S.,
932 Kumar, P., Sahu, R., Navinkumar, P. J., Tanniru, S. R., Javed, A., Soheb, M., Dimri, A. P.,
933 Yadav, M., Devaraju, B., Chinnasamy, P., Reddy, M. J., Murugesan, G. P., Arora, M., Jain,
934 S. K., Ojha, C. S. P., Harrison, S., and Bamber, J.: Challenges in understanding the variability
935 of the cryosphere in the Himalaya and its impact on regional water resources,
936 https://doi.org/10.3389/frwa.2022.909246, 2022.

937 Wagnon, P., Linda, A., Arnaud, Y., Kumar, R., Sharma, P., Vincent, C., Pottakkal, J. G.,
938 Berthier, E., Ramanathan, A., Hasnain, S. I., and Chevallier, P.: Four years of mass balance
939 on Chhota Shigri Glacier, Himachal Pradesh, India, a new benchmark glacier in the western
940 Himalaya, J. Glaciol., 53, 603–611, https://doi.org/10.3189/002214307784409306, 2007.

941 Wagnon, P., Brun, F., Khadka, A., Berthier, E., Shrestha, D., Vincent, C., Arnaud, Y., Six,
942 D., Dehecq, A., Ménégoz, M., and Jomelli, V.: Reanalysing the 2007–19 glaciological mass-
943 balance series of Mera Glacier, Nepal, Central Himalaya, using geodetic mass balance,
944 Journal of Glaciology, 67, 117–125, https://doi.org/10.1017/jog.2020.88, 2021.

945 Yao, J., Chen, Y., Guan, X., Zhao, Y., Chen, J., and Mao, W.: Recent climate and
946 hydrological changes in a mountain–basin system in Xinjiang, China, Earth-Science
947 Reviews, 226, 103957, https://doi.org/10.1016/j.earscirev.2022.103957, 2022.

948 Zemp, M., Thibert, E., Huss, M., Stumm, D., Rolstad Denby, C., Nuth, C., Nussbaumer, S.
949 U., Moholdt, G., Mercer, A., Mayer, C., Joerg, P. C., Jansson, P., Hynek, B., Fischer, A.,
950 Escher-Vetter, H., Elvehøy, H., and Andreassen, L. M.: Reanalysing glacier mass balance
951 measurement series, The Cryosphere, 7, 1227–1245, https://doi.org/10.5194/tc-7-1227-2013,
952 2013.

953 Zemp, M., Frey, H., Gärtner-Roer, I., Nussbaumer, S. U., Hoelzle, M., Paul, F., Haeberli, W.,
954 Denzinger, F., Ahlstrøm, A. P., Anderson, B., Bajracharya, S., Baroni, C., Braun, L. N.,

955 Cáceres, B. E., Casassa, G., Cobos, G., Dávila, L. R., Granados, H. D., Demuth, M. N.,

956 Espizua, L., Fischer, A., Fujita, K., Gadek, B., Ghazanfar, A., Hagen, J. O., Holmlund, P.,

957 Karimi, N., Li, Z., Pelto, M., Pitte, P., Popovnin, V. V., Portocarrero, C. A., Prinz, R.,

958 Sangewar, C. V., Severskiy, I., Sigurðsson, O., Soruco, A., Usubaliev, R., and Vincent, C.:

959 Historically unprecedented global glacier decline in the early 21st century, Journal of

960 Glaciology, 61, 745–762, https://doi.org/10.3189/2015JoG15J017, 2015.

961 Zemp, M., Huss, M., Thibert, E., Eckert, N., McNabb, R., Huber, J., Barandun, M.,

962 Machguth, H., Nussbaumer, S. U., Gärtner-Roer, I., Thomson, L., Paul, F., Maussion, F.,

963 Kutuzov, S., and Cogley, J. G.: Global glacier mass changes and their contributions to sea-

964 level rise from 1961 to 2016, Nature, 568, 382–386, https://doi.org/10.1038/s41586-019-

965 1071-0, 2019.